Surficial-Geologic Reconnaissance and Scarp Profiling on the Collinston and Clarkston Mountain Segments of the Wasatch Fault Zone, Box Elder County, Utah – Paleoseismic Inferences, Implications for Adjacent Segments, and Issues for Diffusion-Equation Scarp-Age Modeling

Paleoseismology of Utah, Volume 15

By
Michael D. Hylland

SPECIAL STUDY 121
UTAH GEOLOGICAL SURVEY
a division of
Utah Department of Natural Resources
2007

Surficial-Geologic Reconnaissance and Scarp Profiling on the Collinston and Clarkston Mountain Segments of the Wasatch Fault Zone, Box Elder County, Utah – Paleoseismic Inferences, Implications for Adjacent Segments, and Issues for Diffusion-Equation Scarp-Age Modeling

Paleoseismology of Utah, Volume 15

By
Michael D. Hylland

ISBN 1-55791-763-9

SPECIAL STUDY 121
UTAH GEOLOGICAL SURVEY
a division of
Utah Department of Natural Resources
2007

STATE OF UTAH
Jon Huntsman, Jr., Governor

DEPARTMENT OF NATURAL RESOURCES
Michael Styler, Executive Director

UTAH GEOLOGICAL SURVEY
Richard G. Allis, Director

PUBLICATIONS
contact
Natural Resources Map/Bookstore
1594 W. North Temple
Salt Lake City, UT 84116
telephone: 801-537-3320
toll-free: 1-888-UTAH MAP
Web site: http://mapstore.utah.gov
email: geostore@utah.gov

THE UTAH GEOLOGICAL SURVEY
contact
1594 W. North Temple, Suite 3110
Salt Lake City, UT 84116
telephone: 801-537-3300
fax: 801-537-3400
Web site: http://geology.utah.gov

Research supported by the U.S. Geological Survey (USGS), Department of the Interior, under USGS award number 03HQAG0008. The views and conclusions contained in this document are those of the author and should not be interpreted as necessarily representing the official policies, either expressed or implied, of the U.S. Government.

Paleoseismology of Utah, Volume 15

FOREWORD

This Utah Geological Survey Special Study, *Surficial-Geologic Reconnaissance and Scarp Profiling on the Collinston and Clarkston Mountain Segments of the Wasatch Fault Zone, Box Elder County, Utah – Paleoseismic Inferences, Implications for Adjacent Segments, and Issues for Diffusion-Equation Scarp-Age Modeling,* is the fifteenth report in the Paleoseismology of Utah series. This series makes the results of paleoseismic investigations in Utah available to geoscientists, engineers, planners, public officials, and the general public. These studies provide critical information regarding paleoearthquake parameters such as earthquake timing, recurrence, displacement, slip rate, and fault geometry, which can be used to characterize potential seismic sources and evaluate the long-term seismic hazard presented by Utah's Quaternary faults.

This report presents the results of a study partially funded through the National Earthquake Hazards Reduction Program to characterize the relative level of activity of the Collinston and Clarkston Mountain segments of the Wasatch fault zone, which is Utah's longest and most active fault. The Collinston and Clarkston Mountain segments are the two northernmost segments of the Wasatch fault zone in Utah. This study involved geologic reconnaissance, scarp-profile measurement and analysis, and empirical analysis of relations between surface rupture length and vertical displacement. Assessing the seismic hazard of the Wasatch fault zone is important because it traverses the most populous part of Utah, with 80 percent of the state's residents living within 10 miles (16 km) of the fault.

Results of this study include estimates of timing of the most recent surface faulting for both segments, and estimates of slip rate and earthquake magnitude for the Clarkston Mountain segment. This report also includes a discussion of issues related to using data from nearby Lake Bonneville shoreline scarps to calibrate diffusion-equation models of fault-scarp age.

William R. Lund, Editor
Paleoseismology of Utah Series

CONTENTS

ABSTRACT 1
INTRODUCTION 1
PREVIOUS WORK 2
GEOLOGIC SETTING 3
COLLINSTON SEGMENT 4
General Description 4
Surficial Geology of the Coldwater Canyon Reentrant 4
Scarp Profiles 6
Fault Scarps 6
Lake Bonneville Shoreline Scarps 8
CLARKSTON MOUNTAIN SEGMENT 9
General Description 9
Surficial Geology of the Elgrove Canyon Area 10
Scarp Profiles and Slip Rate 10
Length-Displacement Relations and Earthquake Magnitude 12
BONNEVILLE SHORELINE SCARP-PROFILE DATA 13
SUMMARY AND CONCLUSIONS 14
ACKNOWLEDGMENTS 16
REFERENCES 16

FIGURES

Figure 1. Index map of Wasatch fault zone 1
Figure 2. Diagrams illustrating fault-scarp nomenclature used in this report 2
Figure 3. Northern segments of the Wasatch fault zone, including the Collinston and Clarkston Mountain segments 3
Figure 4. Surficial-geologic map of the segment boundary between the Collinston and Brigham City segments (Coldwater Canyon reentrant), showing locations of scarp profiles 5
Figure 5. Fault scarps near the mouth of Coldwater Canyon 6
Figure 6. Scarp profiles HVL-1, HVL-2, and HVL-3 in Coldwater Canyon reentrant area 6
Figure 7. Scarp-height – slope-angle relationships for fault scarps and the Bonneville shoreline scarp near Honeyville (Coldwater Canyon reentrant), and the fault scarp at Elgrove Canyon (Clarkston Mountain segment) 8
Figure 8. Scarp profiles HVL-4 and HVL-5 in Coldwater Canyon reentrant area 8
Figure 9. Scarp profiles HVL-8 and HVL-9 in Coldwater Canyon reentrant area 9
Figure 10. Scarp profiles HVL-10 and HVL-11 in Coldwater Canyon reentrant area 9
Figure 11. Scarp profile HVL-12 in Coldwater Canyon reentrant area 9
Figure 12. Scarp profiles HVL-6 and HVL-7 in Coldwater Canyon reentrant area, on Bonneville shoreline scarp 10
Figure 13. Surficial-geologic map of the Elgrove Canyon area near the south end of the Clarkston Mountain segment, showing locations of scarp profiles 11
Figure 14. Fault scarp at the mouth of Elgrove Canyon 12
Figure 15. Scarp profiles EC-1 and EC-2 on fault scarp at mouth of Elgrove Canyon 12
Figure 16. Slope-offset plots showing Lake Bonneville and Lake Lahontan shoreline-scarp data, including data obtained in this study from Bonneville shoreline in Coldwater Canyon reentrant 14

TABLES

Table 1. Scarp-profile data from the Coldwater Canyon/Honeyville and Elgrove Canyon areas 7
Table 2. Estimated surface rupture length for the Clarkston Mountain segment predicted from vertical displacement 13
Table 3. Estimated average and maximum vertical displacements for the Clarkston Mountain segment predicted from surface rupture length 13
Table 4. Comparison of preliminary κ and κ_o values for Bonneville shoreline scarps determined in this study with previously published values 15

Surficial-Geologic Reconnaissance and Scarp Profiling on the Collinston and Clarkston Mountain Segments of the Wasatch Fault Zone, Box Elder County, Utah – Paleoseismic Inferences, Implications for Adjacent Segments, and Issues for Diffusion-Equation Scarp-Age Modeling

By
Michael D. Hylland

ABSTRACT

The Collinston and Clarkston Mountain segments, the northernmost two segments of the Wasatch fault zone in Utah, have been active during the Quaternary Period but show no evidence of Holocene surface faulting. The only fault scarps identified on Quaternary deposits along the Collinston segment are in the area of the Coldwater Canyon reentrant, which is at the segment boundary with the Brigham City segment to the south and includes numerous scarps that resulted at least in part from Holocene Brigham City-segment ruptures. Empirical analysis of scarp-profile data obtained in this study indicates that the timing of the late Holocene most recent surface-faulting earthquake (MRE) in the segment boundary area predates the MRE timing determined in trench studies by others farther south on the Brigham City segment; this suggests the Brigham City-segment MRE identified in the trench studies did not rupture the northernmost part of the Brigham City segment.

The only fault scarp identified on Quaternary deposits along the Clarkston Mountain segment is at Elgrove Canyon, in a reentrant near the south end of the main trace of the segment. Profiles indicate the scarp resulted from two or possibly three surface-faulting earthquakes, each producing approximately 2 m of vertical surface offset. Empirical analysis of the profile data, as well as geologic evidence, indicates the MRE probably occurred shortly prior to the Bonneville highstand of the Bonneville lake cycle. The surface-offset and timing data yield a maximum geologic (open-ended) slip rate of about 0.1 mm/yr for the past 18,000+ years. Empirical relationships between vertical displacement and surface rupture length predict a 30-km-long rupture during a large earthquake on the Clarkston Mountain segment, based on 2 m of per-event vertical displacement at Elgrove Canyon. Surface rupture beyond the mapped main trace during an earthquake could occur on the Short Divide fault or parallel, concealed fault to the south (and possibly both); any concealed southern extension of the main trace of the fault in the valley south of the Short Divide fault; and parts of adjacent segments. Calculations based on displacement and surface rupture length yield an expected earthquake moment magnitude in the range of **M** = 6.8-6.9.

Two profiles across the Bonneville-highstand shoreline scarp in the Coldwater Canyon reentrant provide data for use in calibrating diffusion-equation age determinations of nearby fault scarps. However, several issues complicate the application of these data to diffusion-equation modeling of fault-scarp age, and work to resolve these issues is ongoing.

INTRODUCTION

This report summarizes a non-trenching paleoseismic investigation of the Collinston and Clarkston Mountain segments of the Wasatch fault zone (figure 1). These are the northernmost two segments of the Wasatch fault zone in Utah, and along with the Malad City segment in Idaho, are substantially less active than the more central segments of the fault zone to the south. Whereas the Collinston and Clarkston

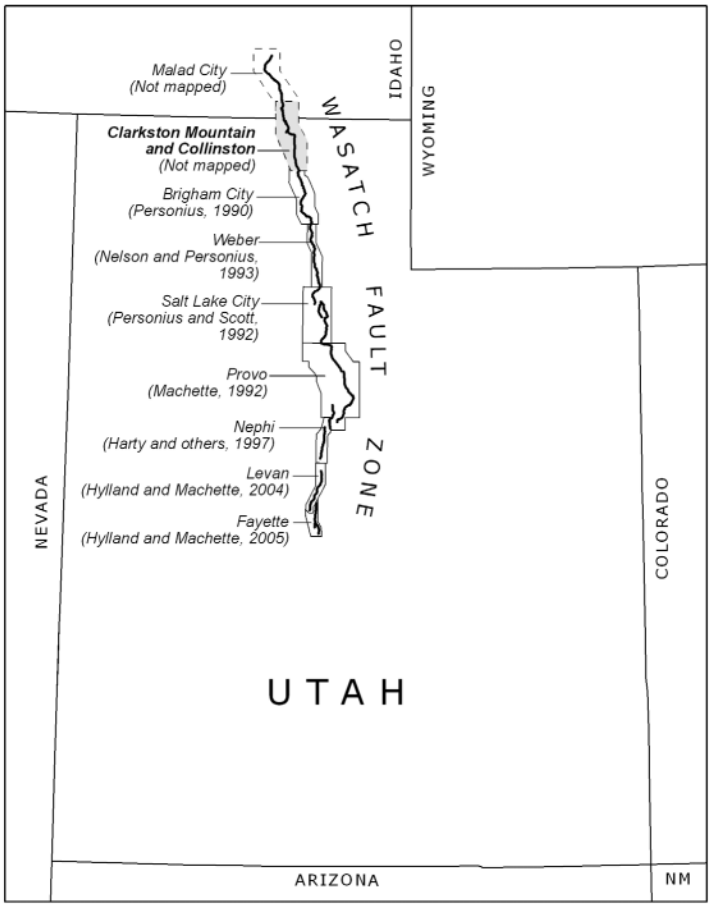

***Figure 1**. Index map of Wasatch fault zone showing segments and published 1:50,000-scale strip maps.*

Mountain segments have been the subject of reconnaissance paleoseismic studies in the past (summarized in Machette and others, 1992a) and have been mapped in the context of 1:24,000-scale geologic quadrangle mapping (Oviatt, 1986a, 1986b; Biek and others, 2003), they have not had any detailed paleoseismic study, primarily owing to the scarcity of Holocene fault scarps and distance from large population centers. The purpose of this investigation is to confirm the presence/absence of fault scarps as determined by previous workers, verify mapped surficial geology in areas where scarps are present, and evaluate the timing of scarp formation using scarp-profile data.

This investigation consisted of a review of published and unpublished geologic mapping along the segments; aerial-photo and field reconnaissance to verify the existing geologic mapping, particularly map relations among Tertiary and Quaternary deposits, fault scarps, and shoreline scarps formed during stillstands of the latest Pleistocene Bonneville lake cycle; and measurement of 14 profiles across fault and shoreline scarps to obtain data for empirical and diffusion-equation age determinations. The scarp profiles were measured using an Abney level and telescoping stadia rod; scarp heights, slope angles, and net surface offsets were determined from computer plots of the scarp profiles. Terminology used to describe fault-scarp morphology, summarized in figure 2, follows that established by Bucknam and Anderson (1979), Machette (1982), and Hanks and others (1984). Metric (SI) units are used throughout this report except for elevations of map features (such as shorelines), which are reported using English units (feet) to be consistent with the base maps.

PREVIOUS WORK

Cluff and others (1974) used low-sun-angle aerial photography and limited field reconnaissance to map lineaments, including fault scarps, along the Wasatch fault zone from Brigham City, Utah, to 4 km northeast of Malad City, Idaho. This part of the Wasatch fault zone was subsequently divided into three segments, primarily on the basis of geomorphic and structural relations: from south to north, the Collin-

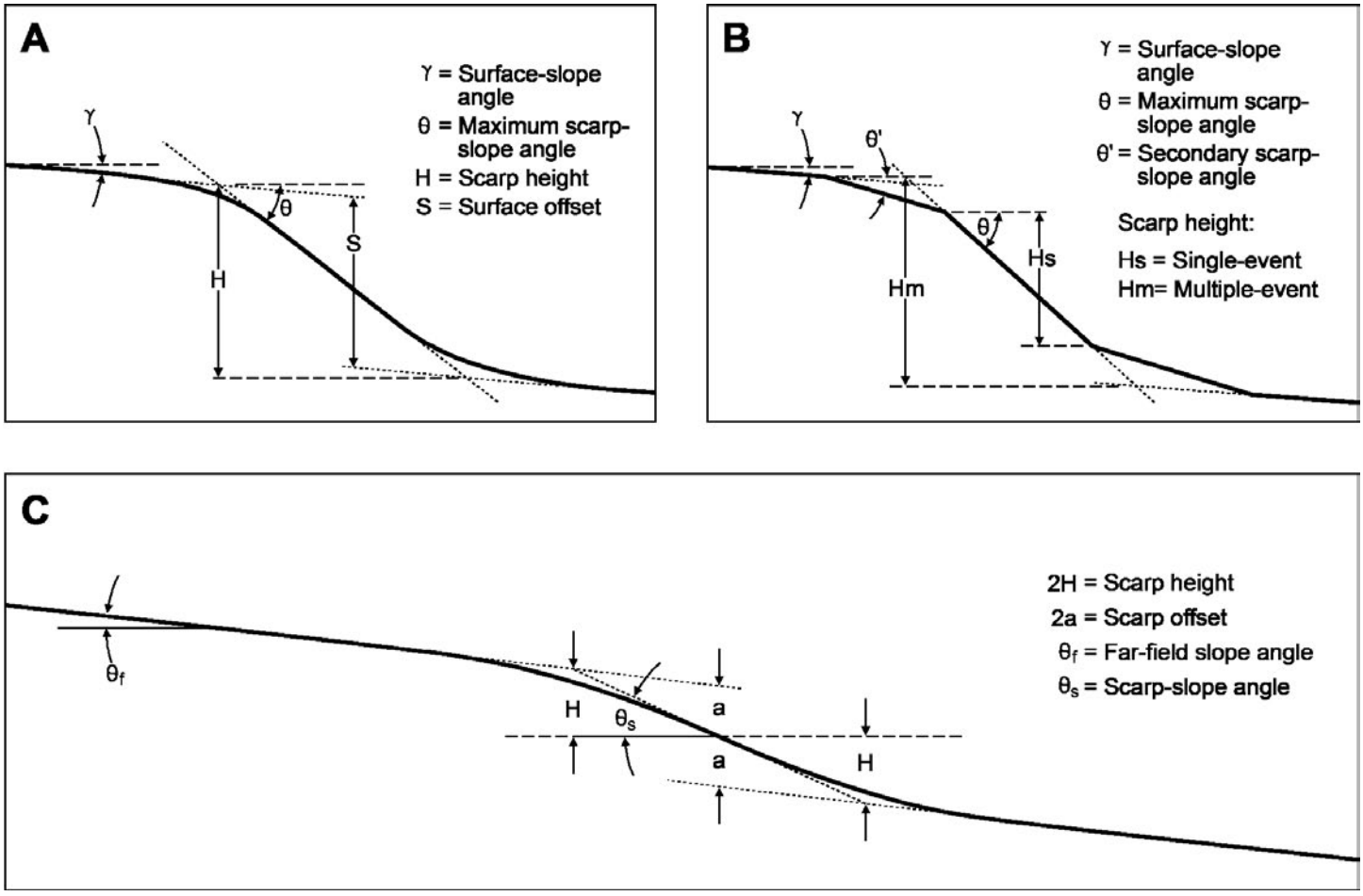

Figure 2. *Schematic diagrams illustrating fault-scarp nomenclature used in this report. (A) Single-event scarp profile and measurements used in empirical scarp-age modeling (modified from Bucknam and Anderson, 1979). (B) Multiple-event scarp profile and measurements used in empirical scarp-age modeling (modified from Machette, 1982). (C) Generalized scarp profile and measurements used in diffusion-equation scarp-age modeling (after Hanks and others, 1984).*

ston, Clarkston Mountain, and Malad City segments (figure 3). Reconnaissance mapping and limited paleoseismic data to the south led Schwartz and Coppersmith (1984) to initially define the Collinston segment as extending approximately 30 km between Brigham City and the town of Collinston. Personius (1990) redefined the south end of the Collinston segment as being located near Honeyville, 12 km north of Brigham City; he included the southern approximately 10 km of the Collinston segment on his 1:50,000-scale surficial-geologic strip map of the Brigham City segment, and measured several scarp profiles in the segment-boundary area. Machette and others (1991, 1992a) subdivided the remaining northern 36 km of the Wasatch fault zone into the Clarkston Mountain segment (19 km) and Malad City segment (17 km), placing the segment boundary at the Woodruff spur in southern Idaho.

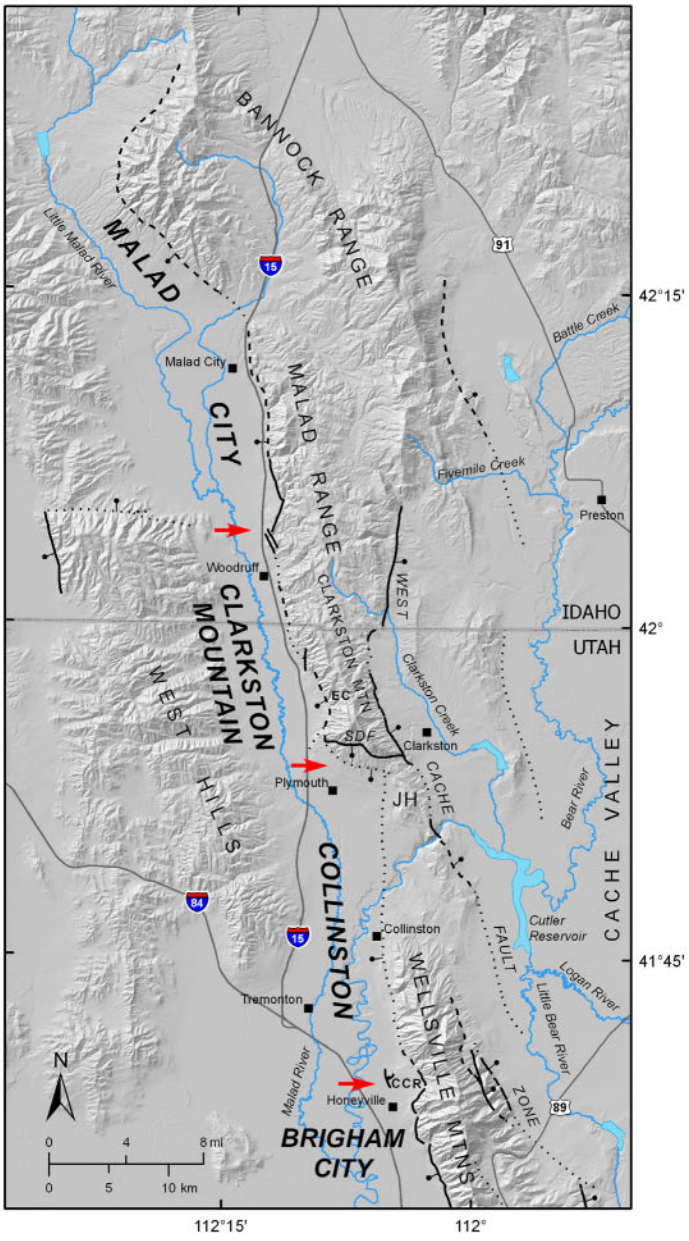

Figure 3. *Northern segments of the Wasatch fault zone (large, bold type), including the Collinston and Clarkston Mountain segments, and other nearby faults having Quaternary movement. Faults shown by heavy lines, dashed where approximately located, dotted where concealed; bar and ball on downthrown side; red arrows show segment boundaries. CCR, Coldwater Canyon reentrant; EC, Elgrove Canyon; JH, Junction Hills; SDF, Short Divide fault. Fault traces after Black and others (2003) (faults in Utah), and U.S. Geological Survey and Idaho Geological Survey (2006) (faults in Idaho).*

Doelling's (1980) 1:125,000-scale geologic map of Box Elder County shows generalized geology along the Collinston and Clarkston Mountain segments. More detailed (1:24,000 scale) geologic maps include those of Oviatt (1986a, 1986b) in the area of the Collinston segment and Biek and others (2003) in the area of the Clarkston Mountain segment.

GEOLOGIC SETTING

The Collinston and Clarkston Mountain segments of the Wasatch fault zone lie along the base of the steep western slopes of the Wellsville Mountains and southern Malad Range (Clarkston Mountain), respectively (figure 3). Bedrock in both ranges consists primarily of Paleozoic sedimentary rocks. A major topographic saddle exists between the northern end of the Wellsville Mountains and southern end of Clarkston Mountain, through which the Bear River flows westward out of Cache Valley into the Great Salt Lake basin. Bedrock in this area, exposed in and adjacent to the Junction Hills, consists of Paleozoic sedimentary rocks and Tertiary basin-fill deposits, the latter of which are typically assigned to the Salt Lake Formation. Outcrops of Salt Lake Formation are also present in the reentrant in the vicinity of Elgrove Canyon near the southern end of Clarkston Mountain. Quaternary deposits along the fault zone include nearshore lacustrine sediments deposited in Lake Bonneville, fan alluvium, talus and colluvium, and mass-movement deposits.

Late Pleistocene Lake Bonneville had a pronounced effect on the surficial geology of the area. Lacustrine sediments and the lake's two highest shoreline complexes are preserved along both the Collinston and Clarkston Mountain segments. As summarized by Currey (1990) and Oviatt and others (1992), the Bonneville lake cycle began around 30 ka. Over time, the lake rose and eventually reached its highest level at the Bonneville shoreline around 18,000 cal yr B.P. (calendar-calibrated radiocarbon ages in this discussion from D.R. Currey, University of Utah, written communication to Utah Geological Survey, 1996). At the Bonneville level, lake water overflowed the low point on the basin rim at Zenda in southeastern Idaho, spilling into the Snake-Colombia River drainage basin. Around 16,800 cal yr B.P., the alluvial-fan deposits at the Zenda outlet failed catastrophically, resulting in a rapid drop in lake level of approximately 100 m associated with the Bonneville Flood. The lake level stabilized when further erosional downcutting was essentially stopped by the bedrock-controlled Red Rock Pass threshold. The lake remained at this

level for possibly over 2500 years (Godsey and Chan, 2005), forming the Provo shoreline. A change in climate to warmer and drier conditions caused the lake to regress rapidly from the Provo shoreline to near modern Great Salt Lake levels by around the beginning of the Holocene.

COLLINSTON SEGMENT

General Description

The extent of the Collinston segment is poorly defined because of the absence of post-Lake Bonneville fault scarps along most of its length (Schwartz and Coppersmith, 1984; Oviatt, 1986a, 1986b; Personius, 1990; Machette and others, 1992a; this study). The southern end of the segment is in a reentrant in the mountain front 2 km northeast of Honeyville (Coldwater Canyon reentrant of Oviatt, 1986a) (figure 3). Here, the trend of the fault changes abruptly, the amount of net surface offset of similar-aged deposits changes substantially, and Holocene fault scarps characteristic of the Brigham City segment to the south are absent to the north (Personius, 1990; Machette and others, 1992a). The northern end of the Collinston segment is generally considered to be in the vicinity of Short Divide at the southern end of Clarkston Mountain (Machette and others, 1992a; Biek and others, 2003) (figure 3), where two down-to-the-south normal faults extend east-west between the Collinston and Clarkston Mountain segments (see "Clarkston Mountain Segment" discussion below).

The topography of the area between the Wellsville Mountains and Clarkston Mountain suggests a south-to-north decrease in total throw on the Collinston segment (Machette and others, 1992a). Machette and others (1992a) proposed the presence of the West Cache fault zone, which lies within 10 km east of the Collinston and Clarkston Mountain segments (figure 3), as a possible explanation for the decrease in throw. The West Cache fault zone has undergone movement in the Holocene (Solomon, 1999; Black and others, 2000), indicating an apparent eastward transfer of extension, or strain partitioning, from the Wasatch fault zone to the West Cache fault zone in the late Quaternary.

A northwest-trending, down-to-the-southwest, low-angle normal fault (Beaver Dam fault; Goessel, 1999; Goessel and others, 1999) is present in the area between the Wellsville Mountains and Clarkston Mountain. This fault extends along the west side of the Junction Hills from the southern end of Clarkston Mountain to the West Cache fault zone at the northeastern end of the Wellsville Mountains, diagonally crossing the topographic divide between Cache Valley and the Great Salt Lake basin. Sprinkel (1976) first described the fault, and cited the apparent juxtaposition of Salt Lake Formation against Lake Bonneville sediments near the south end of the fault as evidence for Late Pleistocene movement. However, Quaternary fault scarps are absent along the entire length of the fault, the inferred trace being concealed beneath lacustrine, landslide, and colluvial deposits (Sprinkel, 1976; Oviatt, 1986b; Biek and others, 2003). If Quaternary movement has occurred along this fault, it may have been subsidiary to primary rupture on the Collinston segment or West Cache fault zone. The Beaver Dam fault has been tentatively proposed as a new segment of the Wasatch fault zone (Goessel, 1999; Goessel and others, 1999). Given the structural uncertainties associated with this fault and the lack of compelling geologic evidence, I do not treat it herein as an independent segment of the Wasatch fault zone, but rather follow the traditional segmentation scheme of Schwartz and Coppersmith (1984) and Machette and others (1992a).

Bonneville-lake-cycle and younger deposits conceal the trace of the Collinston segment along nearly its entire length (Oviatt, 1986a, 1986b; Personius, 1990; Machette and others, 1992a; this study). The only fault scarps on Quaternary deposits that have been reported by previous workers are in the area of the Coldwater Canyon reentrant. Personius (1990) interpreted the northernmost of these fault scarps—an indistinct, eroded, 2-km-long scarp on Bonneville-lake-cycle lacustrine deposits and Provo-aged fan alluvium—as the north end of a Brigham City-segment rupture, and I concur. North of this scarp, isolated outcrops of Paleozoic and Tertiary bedrock west of the main mountain front help to constrain the location of the concealed trace of the Collinston segment, and indicate that the fault lies between the Bonneville and Provo shorelines in several places (Oviatt, 1986a, 1986b). Therefore, the most recent Collinston-segment surface faulting occurred sometime before the Bonneville highstand at 18-16.8 ka. Scarps on Quaternary deposits along the Collinston segment north of the Coldwater Canyon reentrant all appear to be associated with Lake Bonneville shorelines or mass movements. The steep bedrock escarpments along the Wellsville Mountains and Junction Hills to the north suggest that the Collinston segment may have been relatively active in Late Pleistocene time (Machette and others, 1992a).

Surficial Geology of the Coldwater Canyon Reentrant

Quaternary deposits in the general area of the Coldwater Canyon reentrant consist of fan alluvium, lacustrine sediment of the Bonneville lake cycle, hillslope colluvium, and mass-movement deposits (figure 4). As mapped by Personius (1990), the fan alluvium includes two pre-Bonneville units, one Bonneville-aged unit graded to the Provo shoreline, and three post-Bonneville units. The two pre-Bonneville alluvial-fan units (af5 and af4) form high, remnant surfaces at the mouths of Coldwater, Jim May, and Two Jump Canyons. The af5 and af4 surfaces are as high as about 40 m and 20 m, re-

spectively, above adjacent modern stream channels. Soil developed on the af5 deposits is characterized by a strong argillic B horizon and stage III carbonate morphology, and soil developed on the af4 deposits is characterized by a moderate argillic B horizon and stage II-III carbonate morphology; both units are probably of Middle Pleistocene age (Personius, 1990). The Bonneville shoreline, at an altitude of 5200 ft in this area, cuts and forms large scarps on both of these units. At the mouth of Jim May Canyon, two parallel fault scarps form a relatively large graben on the af5 deposits. The main, west-facing scarp is 39 m high, and the net surface offset across the graben is 12 m (Personius, 1990).

The Provo shoreline (figure 4) is at an altitude of about 4800 ft in this area. Alluvial-fan deposits graded to the Provo shoreline (afp) are present in isolated exposures where they have not been buried by younger fan alluvium. Fault scarps on the order of about 10 m high are present on afp deposits at two locations: about 1 km southwest of the mouth of Two Jump Canyon, and midway between the Provo and Bonneville shorelines west of Two Jump Canyon. Most of the ground surface between the Provo and Bonneville shorelines, as well as much of the surface below the Provo shoreline, is covered by unfaulted post-Provo fan alluvium (af2, af1, afy).

Lake Bonneville nearshore sand and gravel deposits are present immediately below the Bonneville (lbg) and Provo (lpg) shorelines (figure 4). Two short, parallel scarps are present on a small exposure of lacustrine sediment, mapped by Oviatt (1986a) and Personius (1990) as shoreline sand and gravel (unit lbg on figure 4), immediately south of the mouth of Coldwater Canyon (figures 4 and 5). Neither Oviatt (1986a) nor Personius (1990) delineated these scarps on their maps. The lower (western) scarp is about 7-9 m high and the upper (eastern) scarp is about 13-15 m high. The scarps are truncated at both ends by Holocene fan alluvium. Given that these scarps are at an elevation between the Bonneville and Provo shorelines, trend slightly oblique to topographic contours, and are on-trend with the 10-m-high fault scarp to the south, I interpret them to be fault scarps rather than lacustrine depositional features such as beach berms. Also, the very coarse (bouldery) nature of the deposits suggests that they may comprise pre-Bonneville-shoreline fan alluvium, possibly correlative with Late Pleistocene fan alluvium (af3) mapped elsewhere along the Wasatch fault zone (see, for example, Nelson and Personius, 1993). The Bonneville sand and gravel deposits appear to form a discontinuous veneer over the older, bouldery deposits.

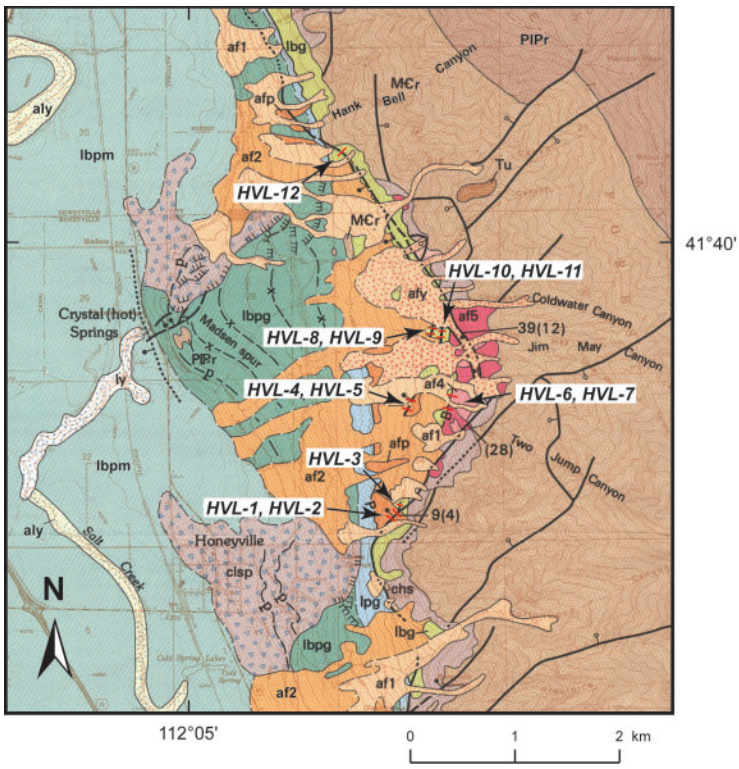

EXPLANATION

aly	Younger stream alluvium (Holocene - uppermost Pleistocene)
ly	Marsh and lacustrine deposits (Holocene - uppermost Pleistocene)
af1	Fan alluvium (upper Holocene)
af2	Fan alluvium (middle Holocene - uppermost Pleistocene)
afy	Younger fan alluvium (Holocene - uppermost Pleistocene)
afp	Fan alluvium related to Provo shorelines (uppermost Pleistocene)
af4	Fan alluvium (upper Middle Pleistocene)
af5	Fan alluvium (Middle Pleistocene)
lpg	Lacustrine sand and gravel related to Provo shorelines (uppermost Pleistocene)
lbg	Lacustrine sand and gravel related to Bonneville shorelines (Upper Pleistocene)
lbpg	Lacustrine sand and gravel related to Provo and Bonneville shorelines (Upper Pleistocene)
lbpm	Lacustrine silt and clay related to Provo and Bonneville shorelines (Upper Pleistocene)
chs	Hillslope colluvium (Holocene to Upper Pleistocene)
clsp	Lateral spread deposits (Holocene to Upper Pleistocene) (reinterpreted by Harty and Lowe [2003] as mass-movement deposits not associated with liquefaction-induced lateral spread)
Tu	Tertiary deposits
PIPr	Lower Permian to Pennsylvanian sedimentary rocks
MCr	Mississippian to Cambrian sedimentary rocks

9(4) — Normal fault - Bar and solid ball on downdropped side along Wasatch fault zone; bar and hollow ball along other faults. Dashed where approximately located, dotted where concealed. Height of fault scarp and amount of geomorphic surface offset (in parentheses) shown in meters (from Personius, 1990). Red line shows location of scarp profile measured in this study

---B--- Major shorelines related to levels of the Bonneville lake cycle - May coincide with geologic contact
B - Highest shoreline of the Bonneville level
P - Highest shoreline of the Provo level
p - Other shorelines of the Provo level (mostly regressive)
x - Undesignated shorelines of the Bonneville lake cycle

Landslide escarpment - Main scarps and fissures; may coincide with geologic contacts

Figure 4. *Surficial-geologic map of the segment boundary between the Collinston and Brigham City segments (Coldwater Canyon reentrant), showing locations of scarp profiles measured in this study (modified from Personius, 1990).*

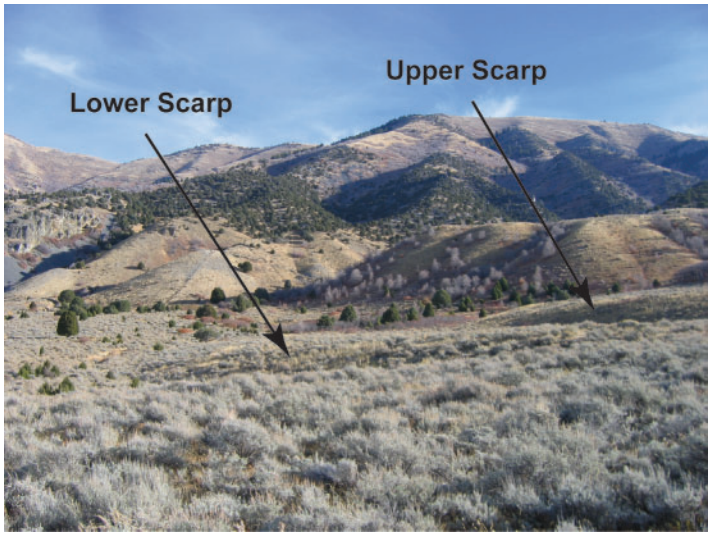

Figure 5. *Fault scarps near the mouth of Coldwater Canyon (view to the northeast). Lower (western) scarp is 7-9 m high and upper (eastern) scarp is 13-15 m high. See scarp profiles HVL-8 through HVL-11 (figures 9 and 10). Elevated surface in mid-ground above upper scarp is underlain by Middle Pleistocene fan alluvium (af5), and surface in foreground is underlain by younger fan alluvium (afy); refer to figure 4.*

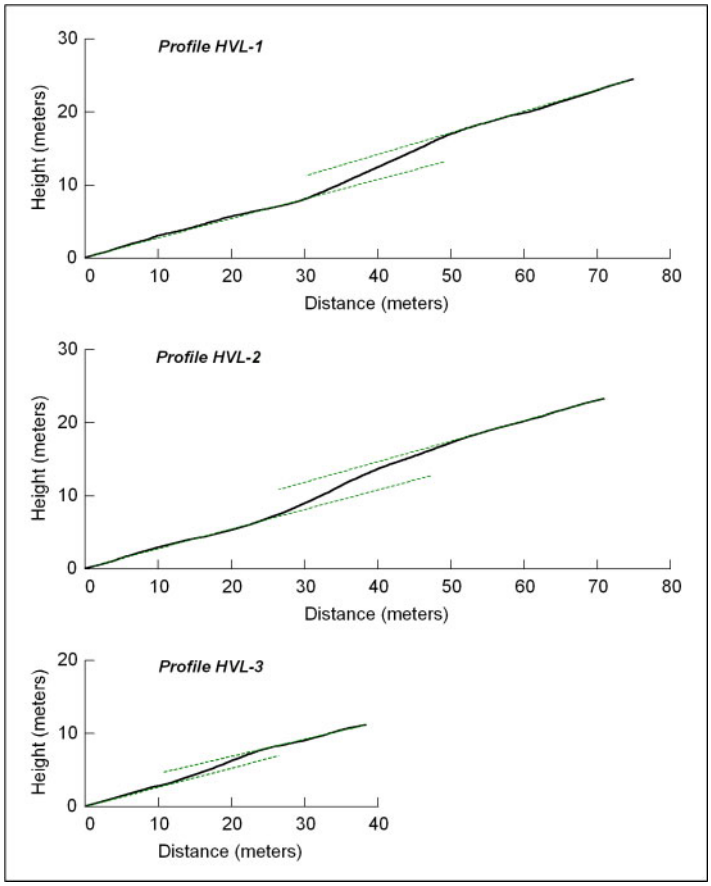

Figure 6. *Scarp profiles in Coldwater Canyon reentrant area near Honeyville, southwest of Two Jump Canyon. Profiles HVL-1 and HVL-2 are on main-trace scarp, and HVL-3 is on splay scarp. Dashed lines show averaged ambient (far-field) surface slope. Profile locations are shown on figure 4, and data are summarized in table 1.*

Scarp Profiles

Fault Scarps

I measured a total of 10 profiles across fault scarps in the Coldwater Canyon/Honeyville area (figure 4): two profiles (HVL-1 and HVL-2) across the main scarp southwest of Two Jump Canyon and a third profile (HVL-3) across a small splay off of the main scarp; two profiles (HVL-4 and HVL-5) across the scarp west of Two Jump Canyon; two profiles across each of the lower (HVL-8 and HVL-9) and upper (HVL-10 and HVL-11) scarps near the mouth of Coldwater Canyon; and one profile (HVL-12) across the northernmost scarp on Quaternary deposits, south of Hank Bell Canyon. Table 1 summarizes the scarp morphometry data. These profiles are intended to provide data, using empirical and diffusion-equation models, to evaluate along-strike temporal variation in rupture patterns by comparing the timing of Brigham City-segment surface faulting in the segment boundary area with that developed from paleoseismic trenching studies to the south (Personius, 1991; McCalpin and Forman, 2002).

Profiles HVL-1 and HVL-2 indicate that the main fault scarp on Provo-aged fan alluvium at the south end of the Coldwater Canyon reentrant likely resulted from two surface-faulting earthquakes (figure 6). The cumulative surface offset of 3.4-3.7 m (table 1) is larger than would be expected from a single faulting event near the end of a segment (mid-segment Holocene surface displacements have averaged about 2-3 m on the central segments of the Wasatch fault zone; Machette and others, 1992a, 1992b; Lund, 2005), and the composite form of profile HVL-2 is consistent with two events. Personius (1990) also profiled this scarp and, based on a calculated 4 m of surface offset, concluded that the scarp resulted from at least two surface-faulting earthquakes. I determined scarp height and maximum scarp-slope angle associated with the most recent event (MRE) and penultimate event (PE) using the two straight-line segments of the scarp face on profile HVL-2, and geologic observations of textural changes in the scarp-face deposits at profile HVL-1 that correspond to the two scarp-face segments of profile HVL-2. Empirical analysis (after Bucknam and Anderson, 1979) of the scarp heights and maximum scarp-slope angles associated with the MRE, as well as those of the single-event splay scarp (profile HVL-3), indicates a mid-Holocene surface-faulting earthquake based on the position of the data points between regression lines for the Fish Springs and Drum Mountains fault scarps (figure 7). Interestingly, the data points plot well below the regression line for the Fish Springs fault scarp, which is known from radiocarbon dating to have formed sometime after 2280±70 ^{14}C yr B.P., perhaps about 2000 years ago (Bucknam and others, 1989). The scarp-height – slope-angle data therefore indicate that the timing of the MRE in the segment-boundary area predates the timing determined for the MRE at the Brigham City trench site 15 km to the south (event Z; 2100±800 cal yr B.P.) (Mc-

Table 1. *Scarp-profile data from the Coldwater Canyon/Honeyville (HVL) and Elgrove Canyon (EC) areas.*

Profile	H_s (m)	H_m (m)	S (m)	θ (°)	θ' (°)	γ (°)	Comments
HVL-1 (full scarp)	-	9.0	3.4	24.5	24.5	16.0	MES (simple morphology)
HVL-1 (MRE)	4.3	-	1.6	24.5	-	16.0	H_s based on field observations
HVL-1 (PE)	4.7	-	1.8	-	24.5	16.0	-
HVL-2 (full scarp)	-	11.7	3.7	27.0	20.0	16.0	MES (pronounced bevel)
HVL-2 (MRE)	5.2	-	1.7	27.0	-	16.0	-
HVL-2 (PE)	6.5	-	2.0	-	20.0	16.0	-
HVL-3	3.0	-	1.0	22.0	-	15.5	SES
HVL-4	-	9.4	5.3	24.0	20.0	10.0	MES (slight bevel)
HVL-5	-	10.5	6.6	24.0	19.0	8.0	MES (slight bevel)
HVL-6	26.5	-	17.0	32.0	-	13.0	Bonneville shoreline scarp
HVL-7	23.0	-	15.8	30.0	-	10.5	Bonneville shoreline scarp
HVL-8	-	8.9	6.6	24.5	21.5, 15.5	4.0	MES (pronounced bevel); min. S
HVL-9	-	7.3	5.7	22.0	15.0	5.0	MES (pronounced bevel); min. S
HVL-10	-	13.4	9.9	25.0	17.5	6.0	MES (pronounced bevel)
HVL-11	-	14.8	11.2	26.0	23.0, 15.5	5.0	MES (pronounced bevel)
HVL-12	3.0	-	1.0	16.0	-	11.5	SES
EC-1 (full scarp)	-	6.2	2.9±1.1	17.5	10.0	4.5 (u), 9.0 (l)	MES (pronounced bevel); min. S
EC-1 (MRE)	2.8	-	~2.1	17.5	-	4.5 (u), 9.0 (l)	Min. S
EC-1 (PE)	3.4	-	~1.9	-	10.0	4.5 (u), 9.0 (l)	May be min. S
EC-2 (full scarp)	-	6.7	3.3±0.8	16.5	13.5	5.5 (u), 9.0 (l)	MES (slight bevel); min. S
EC-2 (MRE)	2.9	-	~1.9	16.5	-	5.5 (u), 9.0 (l)	Min. S
EC-2 (PE)	3.8	-	~2.2	-	13.5	5.5 (u), 9.0 (l)	May be min. S

Symbols and abbreviations:
H_s, scarp height (single-event)
H_m, scarp height (multiple-event)
S, surface offset
θ, maximum scarp-slope angle
θ', secondary scarp-slope angle
γ, ambient (far-field, fan) slope angle
MES, multiple-event scarp
SES, single-event scarp
MRE, most recent event
PE, penultimate event
l, lower fan surface
u, upper fan surface

Calpin and Forman, 2002; Lund, 2005). Apparently the MRE surface rupture documented at the Brigham City trench site did not propagate all the way to the north end of the Brigham City segment.

Profiles HVL-4 and HVL-5 (figure 8) indicate that the scarp on Provo-aged fan alluvium west of Two Jump Canyon likely resulted from at least three surface-faulting earthquakes. Both profiles show composite form, and indicate cumulative surface offset of 5.3-6.6 m (table 1). Scarp heights and maximum scarp-slope angles associated with individual faulting events cannot be distinguished from these profiles with any reasonable degree of confidence, so no empirical analysis was performed using these data.

Profiles HVL-8 and HVL-9 (lower scarp; figure 9) and HVL-10 and HVL-11 (upper scarp; figure 10) indicate that the two parallel scarps on pre-Bonneville fan alluvium (see "Description" discussion above, and figure 5) near the mouth of Coldwater Canyon resulted from numerous surface-faulting earthquakes. The surfaces above and below the upper scarp appear to be correlative, consisting of pre-Bonneville fan alluvium with a veneer of Lake Bonneville sand and gravel. This is not the case for the lower scarp, where the footwall deposits are pre-Bonneville fan alluvium/Bonneville sand and gravel, but the hanging-wall deposits are Holocene fan alluvium. Therefore, the cumulative surface offset of 9.9-11.2 m determined for the upper scarp is representative of total offset, whereas the cumulative surface offset of 5.7-6.6 m determined for the lower scarp is a minimum value of total offset (table 1). The minimum net cumulative surface offset across both faults is approximately 16.7 m. Assuming offset per event is ≤2 m, these two scarps represent at least eight surface-faulting earth-

quakes. For the same reasons given for HVL-4 and HVL-5 in the preceding paragraph, no empirical analysis was performed using the profile data for these scarps. Also, if the faulted deposits are pre-Bonneville in age, and if some of the surface faulting occurred prior to Lake Bonneville reaching this elevation, then transgressional and nearshore lacustrine erosion of the scarp during the Bonneville highstand might have compromised the suitability of the profile data for meaningful diffusion-equation modeling.

Profile HVL-12 (figure 11) is across the relatively obscure fault scarp in the northern part of the Coldwater Canyon reentrant, originally identified by Personius (1990) with the aid of low-sun-angle aerial photos. Although the scarp can be traced over a distance of about 2 km, it is unsuitable for profiling along much of its length due to stream incision, erosion associated with spring discharge, and spatial coincidence with a minor lacustrine shoreline. Where the scarp is relatively well preserved, its height and surface offset (table 1), as well as its simple morphology, indicate it formed as the result of a single surface-faulting earthquake. Empirical analysis of the scarp height and maximum scarp-slope angle indicates latest Pleistocene timing for this earthquake (figure 7); the scarp may represent the northern end of rupture associated with event T on the Brigham City segment, which occurred sometime between 17,000 and 14,800±1200 cal yr B.P. (McCalpin and Forman, 2002; Lund, 2005).

In summary, numerous fault scarps are present in the Coldwater Canyon reentrant, but none can be shown to have formed solely as the result of surface faulting on the Collinston segment. Previous scarp profiling (Personius, 1990) documented a substantial difference in the amount of net surface offset of similar-aged deposits (12 vs. 28 m on scarps on unit af5; see figure 4a), indicating the segment boundary between the Collinston and Brigham City segments is likely at the change in fault trend from northeast (Brigham City) to northwest (Collinston). Scarps in the segment-boundary area on deposits associated with latest Pleistocene Lake Bonneville formed from surface-faulting earthquakes on the Brigham City segment, including the 2-km-long scarp at the southern end of the Collinston segment that has been interpreted as resulting from a Brigham City-segment rupture that spilled over onto the Collinston segment (Personius, 1990). Empirical analysis of scarp-profile data obtained during this study indicates a difference in timing between the Brigham City-segment MRE in the vicinity of the segment boundary and that documented in trench studies 15 km to the south.

Lake Bonneville Shoreline Scarps

A well-developed, erosional, Bonneville-highstand shoreline scarp is present on Middle Pleistocene fan alluvium in the Coldwater Canyon reentrant. I measured two profiles (HVL-6 and HVL-7; figure 12, table 1) across the scarp in the

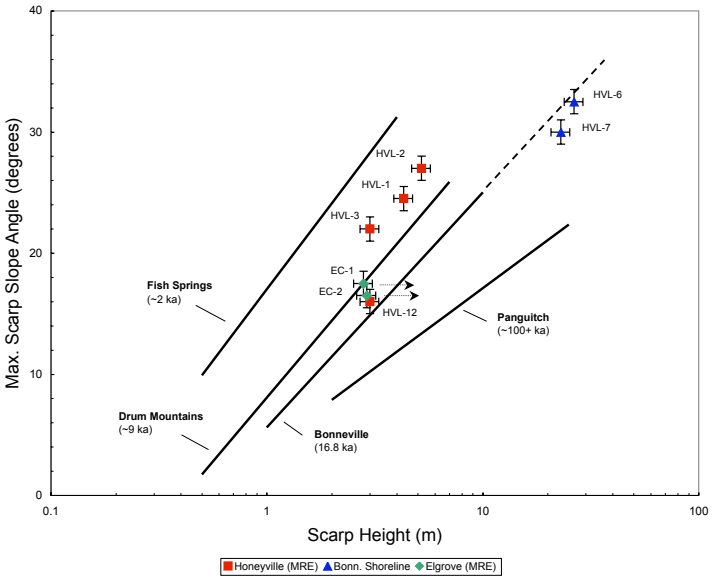

Figure 7. *Scarp-height – slope-angle relationships for fault scarps and the Bonneville shoreline scarp near Honeyville (Coldwater Canyon reentrant), and the fault scarp at Elgrove Canyon (Clarkston Mountain segment). Also shown are best-fit empirical regression lines of Bucknam and Anderson (1979; solid lines) for fault scarps at Fish Springs, Drum Mountains, and Panguitch, Utah, and for shoreline scarps of the Bonneville highstand. Fault-scarp age estimates from Bucknam and others (1989; Fish Springs), Pierce and Colman (1986; Drum Mountains), and Bucknam and Anderson (1979; Panguitch). Dashed part of Bonneville regression line is projected from the Bucknam and Anderson (1979) data. Arrows indicate that scarp height is a minimum value due to partial burial by post-faulting deposition of fan alluvium on the hanging wall. Scarp-profile data are summarized in table 1.*

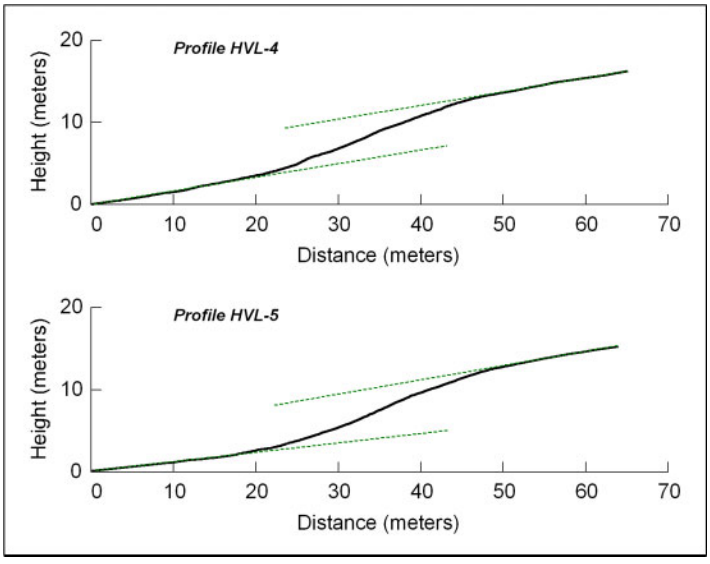

Figure 8. *Scarp profiles HVL-4 and HVL-5 in Coldwater Canyon reentrant area near Honeyville, west of Two Jump Canyon. Dashed lines show averaged ambient (far-field) surface slope. Profile locations are shown on figure 4, and data are summarized in table 1.*

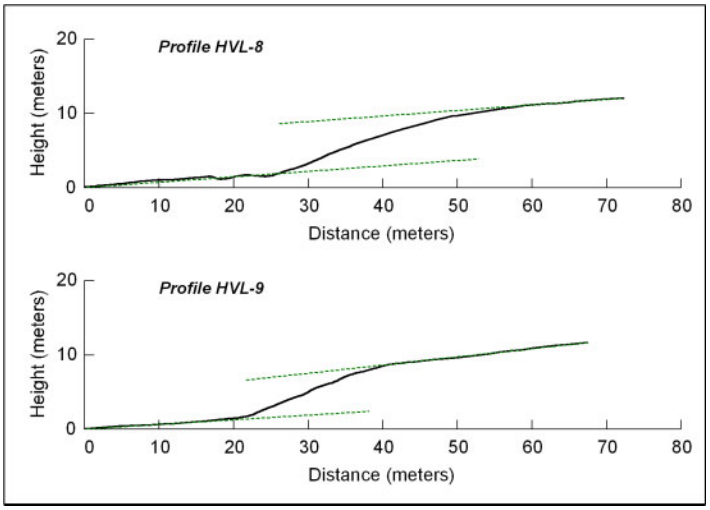

Figure 9. *Scarp profiles HVL-8 and HVL-9 in Coldwater Canyon reentrant area near Honeyville, on lower (western) of two scarps near mouth of Coldwater Canyon. Dashed lines show averaged ambient (far-field) surface slope. Note that deposits underlying footwall and hanging-wall surfaces are not correlative. Profile locations are shown on figure 4, and data are summarized in table 1.*

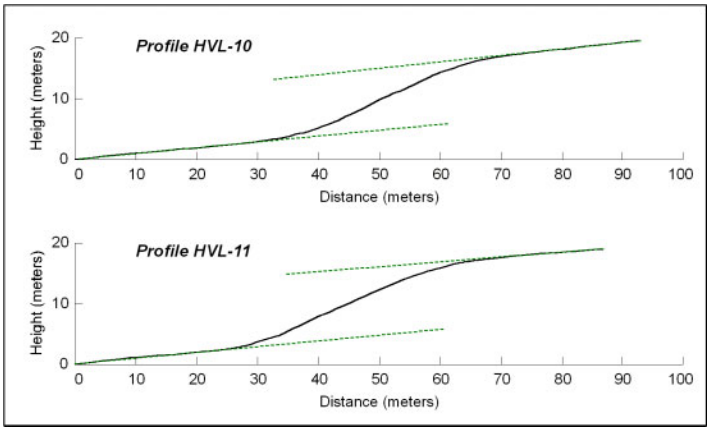

Figure 10. *Scarp profiles HVL-10 and HVL-11 in Coldwater Canyon reentrant area near Honeyville, on upper (eastern) of two scarps near mouth of Coldwater Canyon. Dashed lines show averaged ambient (far-field) surface slope. Profile locations are shown on figure 4, and data are summarized in table 1.*

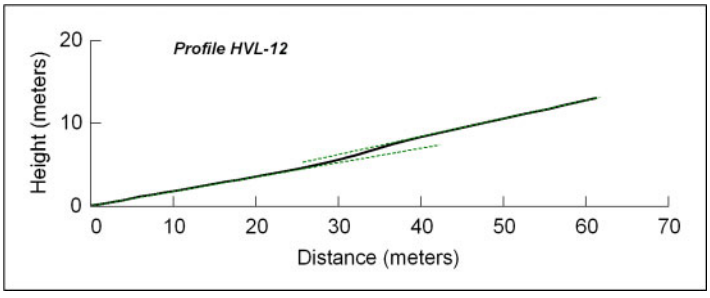

Figure 11. *Scarp profile HVL-12 in Coldwater Canyon reentrant area near Honeyville, south of Hank Bell Canyon. Dashed lines show averaged ambient (far-field) surface slope. Profile locations are shown on figure 4, and data are summarized in table 1.*

vicinity of Two Jump Canyon to provide data for use in calibrating diffusion-equation age determinations of the nearby fault scarps. Several complicating issues exist, however, and work to resolve these issues is ongoing. A discussion of these issues, and preliminary results of the data analysis performed thus far, are presented below under "Bonneville Shoreline Scarp-Profile Data."

CLARKSTON MOUNTAIN SEGMENT

General Description

The Clarkston Mountain segment extends between the southern end of Clarkston Mountain and the Woodruff spur in southern Idaho (Machette and others, 1991, 1992a) (figure 3). The segment boundary between the Clarkston Mountain and Collinston segments is a zone of east-west-trending, down-to-the-south normal faulting that includes the Short Divide fault, which juxtaposes Tertiary Salt Lake Formation strata against lower Paleozoic sedimentary rock. A linear, high (up to 120 m) escarpment subparallel to and about 1 km south of the Short Divide fault is likely a wave-modified fault-line scarp associated with a fault concealed by Bonneville-phase lacustrine sediments, post-Bonneville fan alluvium, and landslide deposits (Biek and others, 2003). The structural block between the Short Divide and concealed faults preserves Salt Lake Formation strata at an intermediate structural level; the youngest faulted unit (tephra subunit of Junction Hills) tephrochronologically correlates with a 7.9±0.5 Ma ash (Biek and others, 2003). Machette and others (1992a) noted that the Short Divide fault appears to have been active as recently as Quaternary time, but post-Salt Lake Formation deposits preserving fault scarps are absent along the fault.

The Woodruff spur is a faulted bedrock spur that extends 6 km along the range front northeast of the town of Woodruff (figure 3). Machette and others (1992a) considered the Woodruff spur to mark the segment boundary between the Clarkston Mountain and Malad City segments based on the complex nature of the fault zone in this area, and coincidence with a transverse structural ridge/gravity saddle (Peterson, 1974; Zoback, 1983).

Bonneville-lake-cycle and younger deposits conceal the trace of the Clarkston Mountain segment along nearly its entire length (Biek and others, 2003; Machette and others, 1992a; this study). The only fault scarp on Quaternary deposits that has been reported by previous workers is at the mouth of Elgrove Canyon near the southern end of the segment (SE1/4NE1/4 section 23, T. 14 N., R. 3 W.). Here, the canyon mouth is above the elevation of the Bonneville shoreline, which in this area is approximately 5150-5180 ft, and the scarp cuts pre-shoreline fan alluvium (Biek and others, 2003). The

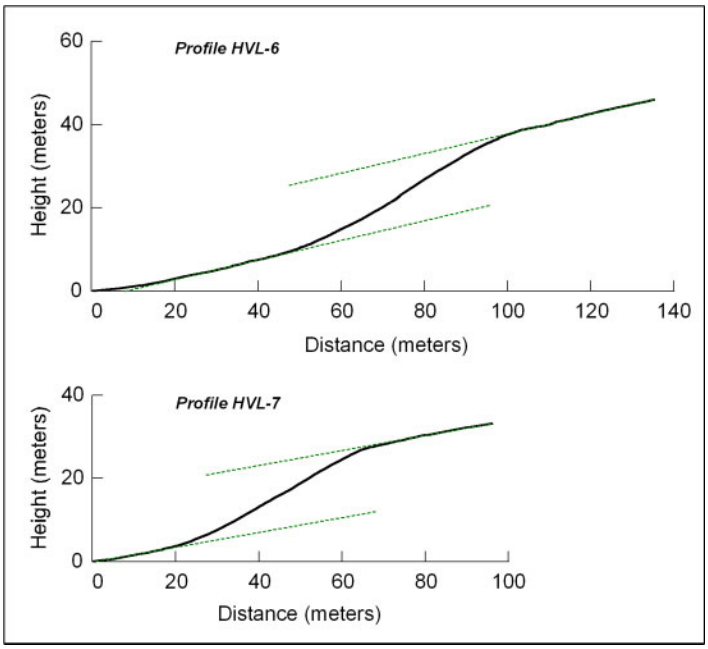

Figure 12. *Scarp profiles HVL-6 and HVL-7 in Coldwater Canyon reentrant area near Honeyville, on Bonneville shoreline scarp near Two Jump Canyon. Dashed lines show averaged ambient (far-field) surface slope. Profile locations are shown on figure 4, and data are summarized in table 1.*

incised stream channel at the south end of the scarp lacks any apparent knickpoint, suggesting a relatively long period of time since scarp formation. The absence of fault scarps on Bonneville-aged or younger deposits elsewhere along the segment indicates the most recent Clarkston Mountain-segment surface faulting occurred sometime before the Bonneville highstand at 18-16.8 ka (Machette and others, 1992a; Biek and others, 2003; this study). Similar to the Wellsville Mountains to the south, the abrupt, linear bedrock escarpment along Clarkston Mountain suggests that the Clarkston Mountain segment may have been relatively active in Late Pleistocene time.

Surficial Geology of the Elgrove Canyon Area

Elgrove Canyon is within a reentrant that is of remarkably similar size and shape to the Coldwater Canyon reentrant described above in the discussion of the Collinston segment. Tertiary and younger deposits in the vicinity of Elgrove Canyon consist of the Salt Lake Formation, fan alluvium, and unmapped deposits of hillslope colluvium and talus (figure 13). As mapped by Biek and others (2003), the fan alluvium includes one unit deposited before and during the Bonneville lake cycle, and two post-Bonneville units. The Bonneville-and-older fan alluvium (Qafo) is preserved as small remnants along the mountain front, including at the mouth of Elgrove Canyon in the footwall of the fault. At Elgrove Canyon, the fan surface is about 5 m above the adjacent modern stream channel. Although I observed no exposures of soil developed on these deposits (and none are reported by Biek and others, 2003), substantial carbonate coatings on clasts at the ground surface indicate the presence of a calcic paleosol of possibly stage II carbonate morphology. Undifferentiated Holocene (post-Bonneville) fan alluvium (Qafy) is present immediately west of the mouth of Elgrove Canyon, and appears to be deposited up against the fault scarp. Late Holocene fan alluvium (Qaf1) bounds the exposure of Qafy on the north and south. The absence of expression of the Bonneville shoreline, either erosionally or depositionally, attests to these deposits being Holocene in age. Steep aprons of talus and colluvium (Qmtc) generally cover the upper parts of these fan deposits adjacent to the bedrock escarpment (Biek and others, 2003).

Although abundant to the north and south, Lake Bonneville deposits are absent in the immediate vicinity of Elgrove Canyon. The Bonneville shoreline has been buried by Holocene alluvial fans across much of the reentrant, and where the shoreline is topographically above the basin-fill/bedrock contact, only small deposits of shoreline sand and gravel remain perched on the steep escarpment. The Provo shoreline, at an altitude of about 4780-4800 ft in this area, is cut on Tertiary Salt Lake Formation, which forms a narrow outcrop belt approximately 0.3 to 1 km west of the mountain front. These exposures of Salt Lake Formation are similar to those south of the Short Divide fault, and indicate the likely presence of a concealed, down-to-the-west normal fault west of the Tertiary outcrops. Biek and others (2003) reported no scarps associated with this fault, and I likewise observed none.

Finally, outcrops of fault breccia are present along the base of the mountain front (figure 13). The well-cemented dolomite breccia forms resistant flatirons and allows direct measurement of fault dip. Biek and others (2003) reported a fault dip of about 45° W. for the Clarkston Mountain segment, and I measured a dip of 44° W. on several flatirons in the vicinity of Elgrove Canyon.

Scarp Profiles and Slip Rate

I measured two profiles across the fault scarp that cuts pre-Bonneville-shoreline fan alluvium at the mouth of Elgrove Canyon (figures 13 and 14). The scarp extends approximately 40 m between the incised stream channel at its south end and the steep colluvial apron with which it merges at its north end. Table 1 summarizes the scarp morphometry data. Several factors make this scarp less-than-ideal for providing reliable data to determine the timing of scarp formation. First, the geomorphic surfaces on the footwall and hanging wall are not correlative; the hanging-wall fan alluvium is younger than that of the footwall. Second, the scarp is at a U.S. Forest Service trailhead, and while there is no evidence of grading, there has undoubtedly been some localized ground disturbance on the hanging wall associated with vehicle parking. Third, a stock-watering tank has been installed at the base of the scarp to make use of a small spring, and there was probably some ground disturbance

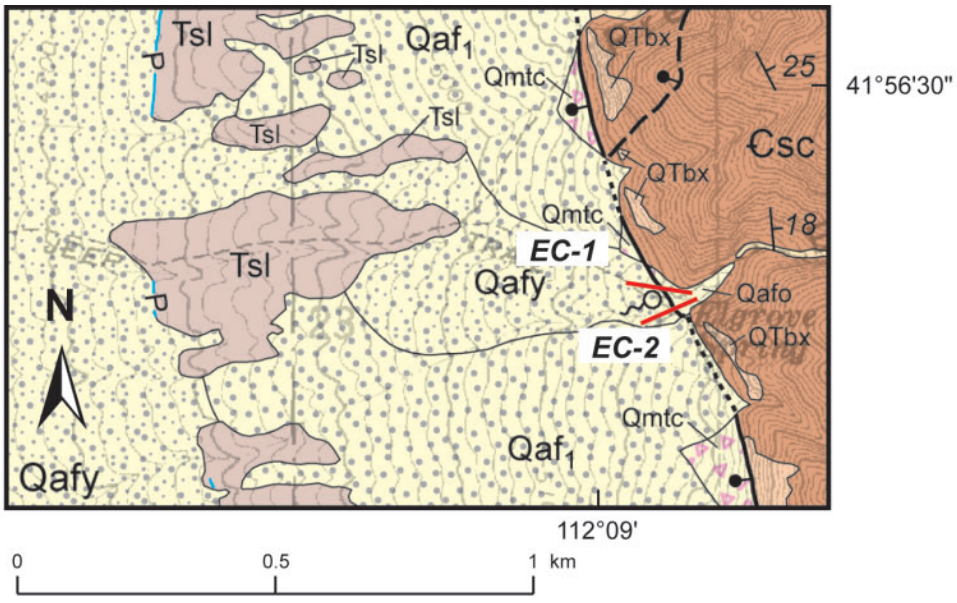

EXPLANATION

Qaf_1	Modern alluvial-fan deposits (upper Holocene)
Qafy	Younger undifferentiated alluvial-fan deposits (Holocene - uppermost Pleistocene)
Qafo	Older alluvial-fan deposits (Upper Pleistocene)
Qmtc	Talus and colluvium (Holocene - Upper Pleistocene)
QTbx	Fault breccia (Pleistocene to Pliocene?)
Tsl	Salt Lake Formation (Pliocene - Miocene)
Csc	St. Charles Formation (Lower Ordovician - Upper Cambrian)

Normal fault - Bar and ball on downdropped side. Dashed where approximately located, dotted where concealed. Red line shows location of scarp profile

P — Highest level of the Provo shoreline of the Bonneville lake cycle - May coincide with geologic contact

25 — Strike and dip of inclined bedding

Spring

Figure 13. *Surficial-geologic map of the Elgrove Canyon area near the south end of the Clarkston Mountain segment, showing locations of scarp profiles measured in this study (modified from Biek and others, 2003).*

on the hanging wall as a result of establishing a level base for the tank. Finally, at least four remains of stone building foundations and other structures are present along the margins of the stream channel near the scarp. These are believed to be pioneer-era (late 1800s) structures used for water storage (Ollie Abusaidi, Caribou National Forest, verbal communication, 2006), and indicate a relatively long period of human activity in the general vicinity of the scarp. Despite these limitations and given the lack of alternative sites, I measured the two profiles across the scarp where ground disturbance appears to be minor to nonexistent.

The profiles (EC-1 and EC-2; figure 15) show a composite scarp morphology resulting from multiple (at least two) surface-faulting events. The profile data indicate a total scarp height of 6.2-6.7 m and a maximum scarp-slope angle of about 17° (table 1). The steepest slope angle is at the base of the scarp, so either the MRE ruptured near the base of the pre-existing scarp, or the ruptures were near the middle of the scarp and the lower part of the scarp associated with the earlier rupture(s) is completely buried. I determined scarp height and maximum scarp-slope angle associated with the MRE and PE (assuming the upper part of the scarp represents a single earlier event) using the two straight-line segments of each profile. Empirical analysis (after Bucknam and Anderson, 1979) of the scarp height and maximum scarp-slope angle associated with the MRE indicates early Holocene timing for this surface-faulting earthquake (figure 7), but this timing estimate is likely a minimum. Part of the total MRE scarp height is likely beneath the surface of the fan alluvium on the hanging wall, so the position of the two data points on figure 7 would shift to the right to represent the true scarp height formed during the surface-faulting earthquake. Timing of the MRE shortly prior to the Bonneville highstand of the Bonneville lake cycle (18-16.8 ka) would be consistent with geologic evidence suggesting that the most recent scarp-forming event predates the end of the Bonneville lake cycle (Machette and others, 1992a; Biek and others, 2003).

Minimum net surface offset across the scarp is between 1.8 and 4.1 m; the large uncertainty is due to the average slope of the fan surface on the hanging wall (~9°) being significantly steeper than that on the footwall (~5°), perhaps associated with footwall erosion. I estimated surface offsets for the MRE and PE (again, assuming the upper part of the scarp represents a single earlier event) by projecting lines from the base and top of the MRE scarp slope, the lines being parallel to the footwall ground surface. This indicates a surface offset of about 2 m for both the MRE and PE (table 1). If the upper part of the scarp is actually the result of two earlier events instead of just one, and an equivalent amount of vertical offset at

the base of the scarp is buried beneath post-faulting alluvium, the per-event surface offset would still be about 2 m.

The lack of any numerical ages to constrain the timing of surface faulting precludes calculation of an accurate slip rate. A maximum geologic (open-ended) slip rate, however, can be estimated using the 2 m of vertical displacement that occurred sometime shortly prior to the Bonneville highstand. This results in an estimated maximum slip rate of about 0.1 mm/yr for the past 18,000+ years.

Length-Displacement Relations and Earthquake Magnitude

The straight-line, end-to-end, surface rupture length (SRL) of the Clarkston Mountain segment is approximately 20 km. This length does not include the Short Divide fault or the parallel, concealed fault to the south. Assuming surface offset measured at Elgrove Canyon provides a reasonably close approximation of vertical fault displacement (throw on fault underestimated by <15%; see, for example, Caskey, 1995), empirical relationships between SRL and displacement (Wells and Coppersmith, 1994) provide insight into the extent of rupture during a surface-faulting earthquake on the segment.

Because of the absence of displacement data from anywhere on the segment other than Elgrove Canyon, it is unclear whether the displacements there are more representative of average or maximum values. The location of Elgrove Canyon near the southern end of the mapped rupture trace (not including the Short Divide fault or parallel, concealed fault) may be justification for considering the inferred 2-m displacements to be more representative of average values; however, given the along-strike variability of vertical displacement typically observed on normal faults, the possibility of the measured displacements representing maximum values cannot be precluded. Table 2 summarizes estimates of SRL predicted from considering 2 m as both an average (AD) and maximum (MD) vertical displacement. Considering 2 m as AD produces a very long SRL relative to the 20-km length of the main trace of the segment. Considering 2 m as MD also produces a long SRL for the segment, but one that is more compatible with the vertical displacement. These results suggest the displacements at Elgrove Canyon may be more representative of MD for the segment than AD. However, these results could also indicate that surface rupture during a large earthquake on the segment may exceed a length of 20 km.

Table 3 summarizes estimates of AD and MD predicted from SRLs of 20 km (approximate length of mapped main trace), 30 km (approximate length predicted from 2-m MD, normal-fault regression), and 40 km (length predicted from 2-m AD, normal-fault regression). The largest estimates of AD, associated with a 40-km SRL, are roughly half of the per-event vertical displacement inferred from the scarp profile data at Elgrove Canyon, whereas the estimated MD for a 30-km SRL (normal-fault regression) is very similar to the inferred per-event vertical displacement. These results further support the hypothesis that vertical displacement at Elgrove Canyon is more representative of MD than AD for the segment. These results also suggest that rupture of just the 20-km main trace of the Clarkston Mountain segment is insufficient to produce the displacements inferred at Elgrove Canyon, and that SRL during a large earthquake may be closer to 30 km. Several possibilities exist where surface rupture could occur beyond the mapped main trace during an earthquake, including the Short Divide fault or parallel, concealed fault (and possibly both);

Figure 14. *Fault scarp at the mouth of Elgrove Canyon, directly behind green stock-watering tank (view to the southeast). Several factors complicate the use of profile data for determining the timing of scarp formation, including ground disturbance of unknown extent associated with use of the site as a trailhead, and installation of the stock-watering tank. Profile EC-1 crosses the scarp to the left of the stock-watering tank, and EC-2 crosses the scarp to the right of the U.S. Forest Service sign, which is approximately 2 m high.*

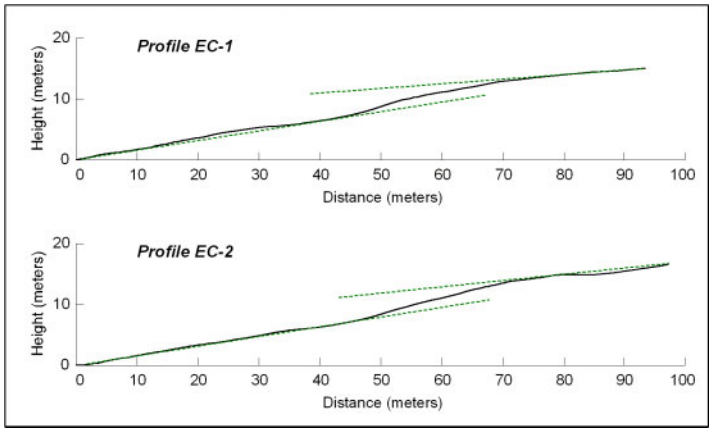

Figure 15. *Scarp profiles EC-1 (northern) and EC-2 (southern) on fault scarp at mouth of Elgrove Canyon. Dashed lines show averaged ambient (far-field) surface slope. Note that deposits underlying footwall and hanging-wall surfaces are not correlative. Profile locations are shown on figure 13, and data are summarized in table 1.*

Table 2. *Estimated surface rupture length (SRL) for the Clarkston Mountain segment predicted from 2 m vertical displacement, considered as average (AD) and maximum (MD) displacements, based on empirical relationships of Wells and Coppersmith (1994).*

Displacement	Fault Type[1]	SRL (km)
AD	Normal	40
	All	60
MD	Normal	29
	All	40

[1] *Normal faults in Wells and Coppersmith database:*
*log (SRL) = 1.52 + 0.28 * log (AD)*
*log (SRL) = 1.36 + 0.35 * log (MD)*
All faults in Wells and Coppersmith database:
*log (SRL) = 1.61 + 0.57 * log (AD)*
*log (SRL) = 1.43 + 0.56 * log (MD)*

Table 3. *Estimated average (AD) and maximum (MD) vertical displacements for the Clarkston Mountain segment predicted from surface rupture length (SRL), based on empirical relationships of Wells and Coppersmith (1994).*

SRL (km)	Fault Type[1]	AD (m)	MD (m)
20	Normal	0.42	0.96
	All	0.52	0.88
30	Normal	0.69	1.8
	All	0.74	1.3
40	Normal	0.99	2.7
	All	0.95	1.8

[1] *Normal faults in Wells and Coppersmith database:*
*log (AD) = -1.99 + 1.24 * log (SRL)*
*log (MD) = -1.98 + 1.51 * log (SRL)*
All faults in Wells and Coppersmith database:
*log (AD) = -1.43 + 0.88 * log (SRL)*
*log (MD) = -1.38 + 1.02 * log (SRL)*

any concealed southern extension of the main trace of the fault in the valley south of the Short Divide fault (e.g., see Biek and others, 2003); and parts of adjacent segments.

In summary, empirical regressions indicate SRL of about 30 km during a large earthquake on the Clarkston Mountain segment, based on 2 m of per-event vertical displacement at Elgrove Canyon. An earthquake associated with 30 km of surface rupture would have an estimated moment magnitude of **M** = 6.8, based on the equations of Wells and Coppersmith (1994) using SRL. Equations using MD = 2 m indicate **M** = 6.8-6.9. These magnitudes compare with **M** = 6.6 resulting from calculations using SRL = 20 km.

BONNEVILLE SHORELINE SCARP-PROFILE DATA

The two profiles (HVL-6 and HVL-7; figure 12) across the Bonneville-highstand shoreline scarp in the Coldwater Canyon/Honeyville area were measured to obtain data for use in calibrating diffusion-equation age determinations of the nearby fault scarps. Applied to landform evolution, the diffusion equation returns the product κt, where the constant of proportionality κ (κ in linear models, κ_o in nonlinear models) is mass diffusivity, and t is time or age (10^3 yr B.P.). If the scarp age is known (e.g., in the case of the Bonneville shoreline scarp), κ or κ_o can be determined. Conversely, if κ or κ_o is known, the timing of scarp formation can be determined. For the shoreline scarp in the Coldwater Canyon/Honeyville area, three issues have emerged that complicate use of the shoreline-scarp profile data in diffusion-equation modeling: (1) the scarp is very high, and has a correspondingly large "surface offset," (2) the scarp slope is relatively steep, and (3) the ambient slope (far-field or fan slope) is relatively steep.

Where the Bonneville shoreline scarp is well developed in the Coldwater Canyon/Honeyville area, it is large (23-26 m high, "surface offset" of 16-17 m), roughly two to four times larger than the profiled fault scarps (table 1). Figures 7 and 16 show the Bonneville shoreline profile data from the Coldwater Canyon/Honeyville area in comparison with previously published Bonneville shoreline datasets. On figure 7, the two Honeyville-scarp data points plot very near the projection (dashed line) of the scarp-height – slope-angle regression line developed for the Bonneville shoreline by Bucknam and Anderson (1979), but are well to the right of the highest scarps used to develop the regression (solid line). Similarly, figure 16 shows that the Honeyville-scarp data points plot well to the right of the Bonneville shoreline scarps having the greatest surface offset ($2a$) in the dataset used to develop the slope-offset plots of Hanks and Andrews (1989). So, with respect to these two Bonneville shoreline datasets, the Honeyville data are outliers. A correction for scarp height will undoubtedly need to be made before the data can be used to calibrate diffusion-equation models for the nearby fault scarps (see, for example, Pierce and Colman, 1986), if they can be used at all (see Nash, 1998).

Hanks and others (1984) showed a dependence of κ on surface offset; in other words, larger values of $2a$ require larger model values of κt (see also Andrews and Bucknam, 1987; Hanks and Andrews, 1989; Hanks, 2000; Mattson and Bruhn, 2001). This dependence is what led to the nonlinear models proposed by Andrews and Bucknam (1987) and Hanks and Andrews (1989). The Andrews and Bucknam (1987) model results in the equation $t = t'(2a)^2/\kappa_o$. The dimensionless age value t' relates maximum scarp slope angle (θ) to ambient (far-field) slope angle (γ) (see discussion in Hanks and

Andrews, 1989), and values of t' have been tabulated for a range of θ and γ (Andrews and Bucknam, 1987, table 2). However, the range of θ assumes an initial scarp slope angle of 31°, and the range of γ has a maximum value of 9°. Also, Andrews and Bucknam (1987) recommended using the tabulated values only for dating scarps with θ = 10°-24°, the range for which their model is well calibrated against data from Bonneville shoreline scarps. These limitations present challenges in using their model to determine the Bonneville shoreline κ_o in the Coldwater Canyon/Honeyville area. In the case of profile HVL-7 (θ = 30°), t' can be extrapolated, as only γ (10°) falls outside the range of tabulated values. For profile HVL-6, however, both θ (32°) and γ (13°) are outside the range of tabulated values.

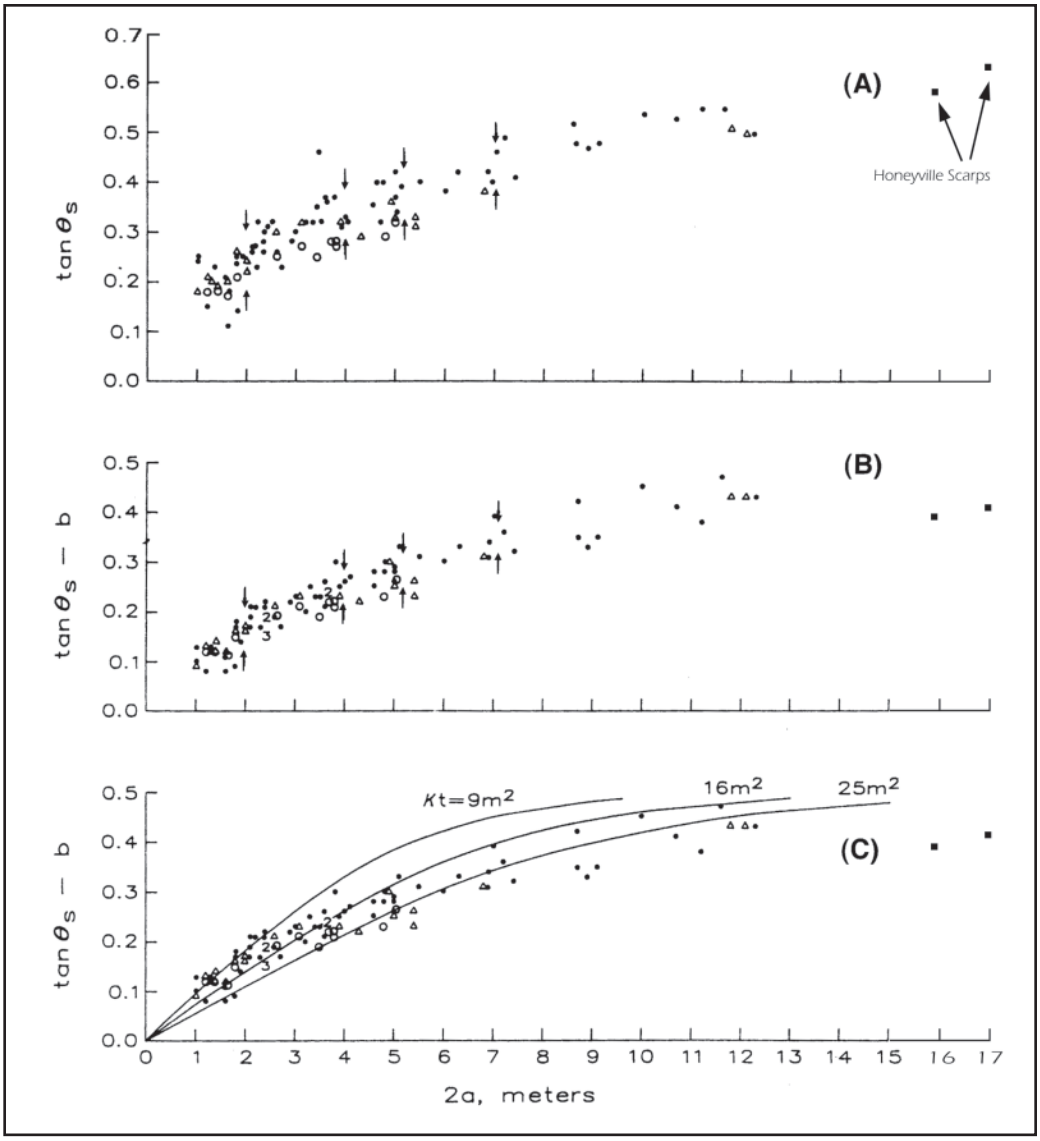

Figure 16. *Slope-offset plots showing Lake Bonneville (solid circles) and Lake Lahontan (open symbols) shoreline-scarp data used by Hanks and Andrews (1989). Solid squares are data obtained in this study from Bonneville shoreline in Coldwater Canyon reentrant near Honeyville. (A) tan θ_s versus 2a, and (B) tan θ_s – b (reduced scarp slope) versus 2a. Arrows on (A) and (B) indicate "full-range" scatter in θ_s for several values of 2a. (C) The data of (B) are shown with three indicated values of κt and (α – b) = 0.5. α, tangent of the angle of repose; b, far-field or fan slope. After Hanks and Andrews (1989).*

Another important consideration related to the Andrews and Bucknam (1987) model is that it is appropriate only for dating single-event scarps. Most of the fault scarps in the Coldwater Canyon/Honeyville area are multiple-event scarps. Mattson and Bruhn (2001) have developed a "constant slip rate" (CSR) solution to diffusion-equation models that can be applied to multiple-event scarps having an unknown rupture history. The CSR solution returns a scarp "initiation age," or time elapsed since slip initiated, as well as an estimate of slip rate that is independent of the age of the offset geomorphic surface (Mattson and Bruhn, 2001; see also DuRoss, 2004, and DuRoss and Bruhn, 2005). Mattson and Bruhn's approach appears to hold promise for quantitative analysis of the fault scarps in the Coldwater Canyon/Honeyville area, but further work is needed to develop appropriate values of κ and κ_o for use in the model.

Table 4 summarizes published κ and κ_o values determined for Bonneville shoreline scarps, as well as preliminary values determined in this study. Hanks and others (1984) and Andrews and Bucknam (1987) used a dataset consisting of 61 Bonneville shoreline triplets ($2a$, θ, and γ), with $2a$ ranging from 1 to 12 m. Their κ and κ_o values were obtained using the radiocarbon age of the Bonneville shoreline (14,500 ^{14}C yr B.P.); I recalculated their values using the calendar-calibrated shoreline age (16,800 cal yr B.P.). Mattson and Bruhn (2001) measured 12 profiles across Bonneville shoreline scarps at four locations, and $2a$ at two of these sites is ≥23 m. The value of κ that I determined for the Honeyville scarp is similar to that determined by Mattson and Bruhn (2001) for the Bonneville shoreline at Tooele, and my κ_o value is similar to that determined by Andrews and Bucknam (1987). Again, the applicability of diffusivity values derived from the large Bonneville shoreline scarp at Honeyville to dating nearby but smaller, multiple-event fault scarps remains uncertain, and the subject of ongoing evaluation and testing.

Table 4. *Comparison of preliminary κ (linear) and κ_o (nonlinear) values for Bonneville shoreline scarps determined in this study with previously published values. N, number of scarp profiles; 2a, scarp "offset" (see figure 2).*

Site	N	*2a* (m)	*κ* (m²/kyr)	κ_o (m²/kyr)	Reference
W. Utah	61	1-12	1.1 [0.95][1]	-	Hanks and others (1984)
W. Utah	61	1-12	-	0.46 [0.39][1]	Andrews and Bucknam (1987)
North Ogden	3	29±3	12.9±1.7	5.9±0.1	Mattson and Bruhn (2001)
South Willow Canyon	4	10±4	1.9±0.5	1.2±0.3	Mattson and Bruhn (2001)
Tooele	2	23	4.7	1.4	Mattson and Bruhn (2001)
Stansbury Mountains	3	4±3	1.8±0.9	1.1±0.4	Mattson and Bruhn (2001)
Honeyville	2	16±1	4.5±0.3[2]	0.55[3]	This study

[1] *Recalculated using calendar-calibrated Bonneville shoreline age.*
[2] *Calculated using equations in Hanks (2000); assumes initial scarp-slope angle of 35°.*
[3] *Calculated using equation in Andrews and Bucknam (1987); data from profile HVL-7.*

SUMMARY AND CONCLUSIONS

The Collinston and Clarkston Mountain segments, the northernmost two segments of the Wasatch fault zone in Utah, are substantially less active than the more central segments of the fault zone to the south. Although apparently relatively more active in Late Pleistocene time, the Collinston and Clarkston Mountain segments show no evidence of Holocene surface faulting. As suggested by Machette and others (1992a), the absence of Holocene movement on the Collinston segment may be related to strain partitioning as reflected by activity on the West Cache fault zone, and the absence of Holocene movement on the Clarkston Mountain segment may be similarly attributed to activity on the West Cache fault zone.

The only fault scarps identified on Quaternary deposits along the Collinston segment are in the area of the Coldwater Canyon reentrant, which is at the segment boundary with the Brigham City segment to the south. The northernmost of these scarps, an indistinct scarp on Bonneville-lake-cycle lacustrine deposits and Provo-aged fan alluvium, appears to be the northern end of a Brigham City-segment rupture. I measured 10 profiles across fault scarps in the Coldwater Canyon reentrant to develop data to evaluate along-strike temporal variation in rupture patterns of the Brigham City segment. All but two of these scarps resulted from multiple surface-faulting earthquakes. Empirical analysis indicates that the timing of the late Holocene most recent event (MRE) in the segment-boundary area predates the timing determined for the MRE at the Brigham City trench site 15 km to the south, suggesting the Brigham City-segment MRE identified in the trench studies did not rupture the northernmost part of the Brigham City segment.

The only fault scarp identified on Quaternary deposits along the Clarkston Mountain segment is at Elgrove Canyon, in a reentrant near the south end of the main trace of the segment. Profiles indicate the scarp on Late Pleistocene fan alluvium is the result of two or possibly three surface-faulting earthquakes, each producing approximately 2 m of vertical surface offset. Empirical analysis indicates the MRE probably occurred shortly prior to the Bonneville highstand of the Bonneville lake cycle (18-16.8 ka), consistent with geologic evidence suggesting that the most recent scarp-forming event predates the end of the Bonneville lake cycle. These data indicate a maximum geologic (open-ended) slip rate of about 0.1 mm/yr for the past 18,000+ years.

Empirical relationships between surface rupture length and vertical displacement provide insight into the extent of rupture during a surface-faulting earthquake on the Clarkston Mountain segment. First, the 2-m-per-event displacements inferred from the scarp-profile data at Elgrove Canyon are more likely representative of maximum displacement than average displacement for the segment. Second, more than just the 20-km main trace likely ruptures during a surface-faulting earthquake on the segment. A modeled maximum displacement of 2 m yields a surface rupture length on the order of 30 km. Surface rupture beyond the mapped main trace during an earthquake could occur on the Short Divide fault or parallel, concealed fault to the south (and possibly both); any concealed southern extension of the main trace of the fault in the valley south of the Short Divide fault; and parts of adjacent segments. The difference in rupture length from 20 to 30 km results in an increase in calculated earthquake moment magnitude from **M** = 6.6 to **M** = 6.8. Earthquake magnitude calculated from 2 m maximum vertical displacement is in the range of **M** = 6.8-6.9.

I measured two profiles across the Bonneville-highstand shoreline scarp in the Coldwater Canyon reentrant to obtain data for use in calibrating diffusion-equation age determinations of nearby fault scarps. Application of the shoreline-scarp profile data to diffusion-equation modeling is complicated, however, by the height of the scarp and correspondingly large "surface offset," the steepness of the scarp slope, and the steepness of the far-field (fan) slope. Preliminary determinations of diffusivity (κ and κ_o) are similar to some published values, but these results will undoubtedly need to be corrected for scarp height before they can be used to calibrate diffusion-equation models for nearby fault scarps, if they can be used at all. The applicability of these preliminary results to diffusion-equation modeling remains the subject of ongoing evaluation and testing.

ACKNOWLEDGMENTS

This study was funded through a cooperative agreement between the Utah Geological Survey (UGS) and U.S. Geological Survey (USGS) (National Earthquake Hazards Reduction Program contract no. 03HQAG0008). Stephen Personius (USGS) provided copies of his interpreted low-sun-angle aerial photographs of the Coldwater Canyon area, and Bob Biek (UGS) discussed his mapping of Clarkston Mountain. Chris DuRoss (UGS) assisted with preliminary diffusion-equation modeling and provided a critical review of this report. Gary Christenson, Bill Lund, and Robert Ressetar (UGS) also provided helpful review comments. Jim Parker and Lucas Shaw (UGS) assisted with figure preparation, and Liz Paton did the manuscript design and layout.

REFERENCES

Andrews, D.J., and Bucknam, R.C., 1987, Fitting degradation of shoreline scarps by a nonlinear diffusion model: Journal of Geophysical Research, v. 92, no. B12, p. 12,857-12,867.

Biek, R.F., Oaks, R.Q., Jr., Janecke, S.U., Solomon, B.J., and Swenson Barry, L.M., 2003, Geologic maps of the Clarkston and Portage quadrangles, Box Elder and Cache Counties, Utah and Franklin and Oneida Counties, Idaho: Utah Geological Survey Map 194, 41 p. pamphlet, 3 plates, scale 1:24,000.

Black, B.D., Giraud, R.E., and Mayes, B.H., 2000, Paleoseismic investigation of the Clarkston, Junction Hills, and Wellsville faults, West Cache fault zone, Cache County, Utah: Utah Geological Survey Special Study 98, Paleoseismology of Utah, v. 9, 23 p.

Black, B.D., Hecker, S., Hylland, M.D., Christenson, G.E., and McDonald, G.N., 2003, Quaternary fault and fold database and map of Utah: Utah Geological Survey Map 193DM, compact disc.

Bucknam, R.C., and Anderson, R.E., 1979, Estimation of fault-scarp ages from a scarp-height – slope-angle relationship: Geology, v. 7, p. 11-14.

Bucknam, R.C., Crone, A.J., and Machette, M.N., 1989, Characteristics of active faults, *in* Jacobson, J.L., compiler, National Earthquake Hazards Reduction Program, Summaries of technical reports, volume XXVIII: U.S. Geological Survey Open-File Report 89-453, p. 117.

Caskey, S.J., 1995, Geometric relations of dip slip to a faulted ground surface – New nomograms for estimating components of fault displacement: Journal of Structural Geology, v. 17, no. 8, p. 1197-1202.

Cluff, L.S., Glass, C.E., and Brogan, G.E., 1974, Investigation and evaluation of the Wasatch fault north of Brigham City and Cache Valley faults, Utah and Idaho – A guide to land-use planning with recommendations for seismic safety: Oakland, California, unpublished consultant's report prepared for the U.S. Geological Survey, 147 p., 1 appendix, 25 sheets, scale 1:24,000.

Currey, D.R., 1990, Quaternary paleolakes in the evolution of semidesert basins, with special emphasis on Lake Bonneville and the Great Basin, U.S.A.: Palaeogeography, Palaeoclimatology, Palaeoecology, v. 76, p. 189-214.

Doelling, H.H., 1980, Geology and mineral resources of Box Elder County, Utah: Utah Geological and Mineral Survey Bulletin 115, 251 p., 3 plates, scale 1:125,000.

DuRoss, C.B., 2004, Spatial and temporal trends of surface rupturing on the Nephi segment of the Wasatch fault, Utah – Implications for fault segmentation and the recurrence of paleoearthquakes: Salt Lake City, University of Utah, M.S. thesis, 120 p.

DuRoss, C.B., and Bruhn, R.L., 2005, Active tectonics of the Nephi segment, Wasatch fault, Utah, *in* Lund, W.R., editor, Western States Seismic Policy Council, Proceedings Volume, Basin and Range Province Seismic Hazards Summit II: Utah Geological Survey Miscellaneous Publication 05-2, 25 p., compact disc.

Godsey, H.S., and Chan, M.A., 2005, New evidence for an extended occupation of the Provo shoreline and implications for paleoenvironmental change from Pleistocene Lake Bonneville, Utah [abs.]: Geological Society of America Abstracts with Programs, v. 37, no. 7, paper no. 148-5, p. 335.

Goessel, K.M., 1999, Tertiary stratigraphy and structural geology, Wellsville Mountains to Junction Hills, north-central Utah: Logan, Utah State University, M.S. thesis, 231 p., 4 plates.

Goessel, K.M., Oaks, R.Q., Jr., Perkins, M.E., and Janecke, S.U., 1999, Tertiary stratigraphy and structural geology, Wellsville Mountains to Junction Hills, north-central Utah, *in* Spangler, L.E., and Allen, C.J., editors, Geology of northern Utah and vicinity: Utah Geological Association Publication 27, p. 45-69.

Hanks, T.C., 2000, The age of scarplike landforms from diffusion-equation analysis, *in* Noller, J.S., Sowers, J.M., and Lettis, W.R., editors, Quaternary geochronology – Methods and applications: American Geophysical Union, AGU Reference Shelf 4, p. 313-338.

Hanks, T.C., and Andrews, D.J., 1989, Effect of far-field slope on morphologic dating of scarplike landforms: Journal of Geophysical Research, v. 94, no. B1, p. 565-573.

Hanks, T.C., Bucknam, R.C., Lajoie, K.R., and Wallace, R.E., 1984, Modification of wave-cut and faulting-controlled landforms: Journal of Geophysical Research, v. 89, no. B7, p. 5771-5790.

Harty, K.M., and Lowe, M., 2003, Geologic evaluation and hazard potential of liquefaction-induced landslides along the Wasatch Front, Utah: Utah Geological Survey Special Study 104, 40 p., 16 plates.

Harty, K.M., Mulvey, W.E., and Machette, M.N., 1997, Surficial geologic map of the Nephi segment of the Wasatch fault zone, eastern Juab County, Utah: Utah Geological Survey Map 170, 14 p., scale 1:50,000.

Hylland, M.D., and Machette, M.N., 2004, Interim surficial geologic map of the Levan segment of the Wasatch fault zone, Juab and Sanpete Counties, Utah, *in* Christenson, G.E., Ashland, F.X., Hylland, M.D., McDonald, G.N., and Case, B., Database compilation, coordination of earthquake-hazards mapping, and study of the Wasatch fault and earthquake-induced landslides, Wasatch Front, Utah: Utah Geological Survey, Final Technical Report to the U.S. Geological Survey, National Earthquake Hazards Reduction Program, award no. 03HQAG0008, 30 p., scale 1:50,000, compact disk.

—2005, Interim surficial geologic map of the Fayette segment of the Wasatch fault zone, Juab and Sanpete Counties, Utah, *in* Christenson, G.E., Hylland, M.D., Lund, W.R., DuRoss, C.B., and McDonald, G.N., Earthquake working groups, database updates, and paleoseismic fault studies, Utah: Utah Geological Survey, Final Technical Report to the U.S. Geological Survey, National Earthquake Hazards Reduction Program, award no. 03HQAG0008, 28 p., scale 1:50,000, compact disk.

Lund, W.R., 2005, Consensus preferred recurrence-interval and vertical slip-rate estimates – Review of Utah paleoseismic-trenching data by the Utah Quaternary Fault Parameters Working Group: Utah Geological Survey Bulletin 134, compact disk.

Machette, M.N., 1982, Quaternary and Pliocene faults in the La Jencia and southern part of the Albuquerque-Belen basins, New Mexico – Evidence of fault history from fault scarp morphology and Quaternary history, *in* Grambling, J.A., and Wells, S.G., editors, Albuquerque Country II: New Mexico Geological Society Guidebook, 33rd Field Conference, p. 161-169.

—1992, Surficial geologic map of the Wasatch fault zone, eastern part of Utah Valley, Utah County and parts of Salt Lake and Juab Counties, Utah: U.S. Geological Survey Miscellaneous Field Investigations Series Map I-2095, scale 1:50,000.

Machette, M.N., Personius, S.F., and Nelson, A.R., 1992a, Paleoseismology of the Wasatch fault zone – A summary of recent investigations, interpretations, and conclusions, *in* Gori, P.L., and Hays, W.W., editors, Assessment of regional earthquake hazards and risk along the Wasatch Front, Utah: U.S. Geological Survey Professional Paper 1500-A, 71 p.

—1992b, The Wasatch fault zone, U.S.A.: Annales Tectonicae, Special Issue – Supplement to Volume VI, p. 5-39.

Machette, M.N., Personius, S.F., Nelson, A.R., Schwartz, D.P., and Lund, W.R., 1991, The Wasatch fault zone, Utah – Segmentation and history of Holocene earthquakes: Journal of Structural Geology, v. 13, no. 2, p. 137-149.

Mattson, A., and Bruhn, R.L., 2001, Fault slip rates and initiation age based on diffusion equation modeling – Wasatch fault zone and eastern Great Basin: Journal of Geophysical Research, v. 106, no. B7, p. 13,739-13,750.

McCalpin, J.P., and Forman, S.L., 2002, Post-Provo paleoearthquake chronology of the Brigham City segment, Wasatch fault zone, Utah: Utah Geological Survey Miscellaneous Publication 02-9, Paleoseismology of Utah, v. 11, 46 p.

Nash, D.B., 1998, Influence of scarp height on the accuracy of morphologic dating [abs.]: Online, Geological Society of America, Annual Meeting, abstract no. 51316, <http://rock.geosociety.org/absindex/annual/1998/51316.htm>.

Nelson, A.R., and Personius, S.F., 1993, Surficial geologic map of the Weber segment, Wasatch fault zone, Weber and Davis Counties, Utah: U.S. Geological Survey Miscellaneous Field Investigations Series Map I-2199, scale 1:50,000.

Oviatt, C.G., 1986a, Geologic map of the Honeyville quadrangle, Box Elder and Cache Counties, Utah: Utah Geological and Mineral Survey Map 88, 13 p., scale 1:24,000.

—1986b, Geologic map of the Cutler Dam quadrangle, Box Elder and Cache Counties, Utah: Utah Geological and Mineral Survey Map 91, 7 p., scale 1:24,000.

Oviatt, C.G., Currey, D.R., and Sack, D., 1992, Radiocarbon chronology of Lake Bonneville, eastern Great Basin, USA: Palaeogeography, Palaeoclimatology, Palaeoecology, v. 99, p. 225-241.

Personius, S.F., 1990, Surficial geologic map of the Brigham City segment and adjacent parts of the Weber and Collinston segments, Wasatch fault zone, Box Elder and Weber Counties, Utah: U.S. Geological Survey Miscellaneous Investigations Series Map I-1979, scale 1:50,000.

—1991, Paleoseismic analysis of the Wasatch fault zone at the Brigham City trench site, Brigham City, Utah and Pole Patch trench site, Pleasant View, Utah: Utah Geological and Mineral Survey Special Study 76, 39 p.

Personius, S.F., and Scott, W.E., 1992, Surficial geologic map of the Salt Lake City segment and parts of adjacent segments of the Wasatch fault zone, Davis, Salt Lake, and Utah Counties, Utah: U.S. Geological Survey Miscellaneous Field Investigations Series Map I-2106, scale 1:50,000.

Peterson, D.L., 1974, Bouguer gravity map of part of the northern Lake Bonneville basin, Utah and Idaho: U.S. Geological Survey Miscellaneous Field Studies Map MF-627, scale 1:250,000.

Pierce, K.L., and Colman, S.M., 1986, Effect of height and orientation (microclimate) on geomorphic degradation rates and processes, late-glacial terrace scarps in central Idaho: Geological Society of America Bulletin, v. 97, no. 7, p. 869-885.

Schwartz, D.P., and Coppersmith, K.J., 1984, Fault behavior and characteristic earthquakes – Examples from the Wasatch and San Andreas fault zones: Journal of Geophysical Research, v. 89, no. B7, p. 5681-5698.

Solomon, B.J., 1999, Surficial geologic map of the West Cache fault zone and nearby faults, Box Elder and Cache Counties, Utah: Utah Geological Survey Map 172, 21 p, scale 1:50,000.

Sprinkel, D.A., 1976, Structural geology of Cutler Dam quadrangle and northern part of Honeyville quadrangle, Utah: Logan, Utah State University, M.S. thesis, 58 p., 2 plates.

U.S. Geological Survey and Idaho Geological Survey, 2006, Quaternary fault and fold database for the United States: Online, U.S. Geological Survey, <http//earthquakes.usgs.gov/regional/qfaults/>, accessed January 2006.

Wells, D.L., and Coppersmith, K.J., 1994, New empirical relationships among magnitude, rupture length, rupture width, rupture area, and surface displacement: Bulletin of the Seismological Society of America, v. 84, no. 4, p. 974-1002.

Zoback, M.L., 1983, Structure and Cenozoic tectonism along the Wasatch fault zone, Utah, *in* Miller, D.M., Todd, V.R., and Howard, K.A., editors, Tectonic and stratigraphic studies in the eastern Great Basin: Geological Society of America Memoir 157, p. 3-27.